# APPENDIX B

# SUMMARY OF RECENT INFORMATION RELEVANT TO THE UNSATURATED ZONE FLOW AND TRANSPORT PROCESS MODEL

INTENTIONALLY LEFT BLANK

# SUMMARY OF RECENT INFORMATION RELEVANT TO THE UNSATURATED ZONE FLOW AND TRANSPORT PROCESS MODEL

## 1. INTRODUCTION

This white paper contains a summary of recent test results and other additional information that are relevant to the unsaturated zone flow and transport process model used to support the *Yucca Mountain Science and Engineering Report* (YMS&ER) (DOE 2001a) and the *Yucca Mountain Preliminary Site Suitability Evaluation* (YMPSSE) (DOE 2001b). The U.S. Department of Energy (DOE) released these two documents for public review in May and August, respectively, of this year.

The white paper focuses on the results of those field and laboratory tests and other additional information that became available after the unsaturated zone flow and transport process model was completed to support the preparation of the YMS&ER and the YMPSSE. The summary of this recent information is being used to conduct an impact review, in accordance with AP-2.14Q, *Review of Technical Products and Data*, to determine if this additional information has any impact on the technical analyses supporting the YMS&ER and the YMPSSE. The documentation of the additional information in this white paper is an interim step, and primarily used to support this impact review. This information is expected to be formally documented in subsequent Project technical reports, as appropriate.

To assist in the impact review, this white paper briefly describes the unsaturated zone flow and transport process model that was used to support the YMS&ER and the YMPSSE, provides a summary of the recent test results and other additional information, and discusses the potential implications of recent information on our understanding of the unsaturated zone flow and transport process model.

## 2. SUMMARY DESCRIPTION OF THE UNSATURATED ZONE FLOW AND TRANSPORT PROCESS MODEL

The unsaturated zone flow and transport model used to support the YMS&ER (DOE 2001a) and YMPSSE (DOE 2001b) is a representation of the water movement affected by climate above the unsaturated zone, rock hydrologic properties of tuff matrix, fractures, and faults above the water table and thermal impacts controlled by the design of the potential repository. The understanding of the water movement through the unsaturated zone is described at length in the *Unsaturated Zone Flow and Transport Model Process Model Report* (CRWMS M&O 2000a) which is supported by 24 detailed analysis and model reports.

The integrated unsaturated zone flow and transport model is comprised of four major components: (1) unsaturated zone flow, (2) drift seepage, (3) drift-scale coupled thermal-hydrologic-chemical processes, and (4) unsaturated zone transport.

### 2.1 UNSATURATED ZONE FLOW

The unsaturated zone flow model is a three-dimensional, site-scale numerical model that simulates groundwater flow from the surface of the mountain to the water table using a dual-permeability formulation to capture flow through fracture and matrix materials. The model

is generated based on information from the geologic framework model, rock properties model, and mineralogical model. It is calibrated and tested against relevant data that include perched-water data, matrix saturation, moisture potential, pneumatic data, air-permeability data, temperature data, and ambient geochemistry data. The three-dimensional flow model is also validated through percolation tests performed in Alcove 1 and comparisons to data from the ECRB, SD-6 and WT-24.

Additional submodels that provide input to the flow model include climate and infiltration models as well as the mountain-scale thermal-hydrologic model. The climate model provides upper and lower bounds for precipitation and temperature for modern and future climates. The timing of the climate states following postclosure are deterministically prescribed and assumed to be as follows: (1) a modern climate lasting for 600 years; (2) a monsoon climate from 600 years to 2,000 years; and (3) a glacial-transition climate for the remainder of the simulated 10,000-year period. The infiltration model uses the precipitation and temperature data from the climate model, along with other inputs such as hydraulic permeability and soil depth, to determine the amount of net infiltration that penetrates beneath the surface of the mountain.

The infiltration model implements a mass balance among flow processes at the surface such as precipitation, evapotranspiration, run-on, run-off, and net infiltration.

The mountain-scale thermal-hydrologic model consists of two- and three-dimensional submodels of the unsaturated zone flow model that include refinement around the repository to accommodate thermal loading. Temperatures and hydrologic conditions are simulated to determine the impact of repository heating on far-field flow.

## 2.2 DRIFT SEEPAGE

The drift-scale seepage models consist of a sequence of models that are used to estimate the amount of water that can enter the waste emplacement drifts under a variety of conditions. The first model in the sequence of seepage models is the seepage calibration model. The seepage calibration model is a three-dimensional heterogeneous fracture-continuum numerical model that contains small-scale variability and correlation structure in the hydrologic properties. The input parameters include permeabilities from air-injection tests and other hydrologic parameters from the calibrated properties model.

The second model is the seepage model for performance assessment. The seepage model for performance assessment is a three-dimensional, heterogeneous fracture-continuum numerical model that uses the conceptual model from the seepage calibration model as its basis. It implements a broader range of parameters from available data as well as drift-degradation scenarios. The seepage model for performance assessment considers variations in percolation flux, permeability, and capillarity (van Genuchten $\alpha$).

The wide range of seepage rates calculated from the seepage model for performance assessment are then used in a performance assessment abstraction model that creates distributions for seepage fraction, mean seep flow rate, standard deviation of seep flow rate, and a flow-focusing factor. The flow-focusing factor is based on estimates of discrete “weep” spacings implied by

the active fracture model and percolation fluxes calculated by the flow model. It is used to scale the percolation flux and the seepage fraction.

## 2.3 DRIFT-SCALE THERMAL-HYDROLOGIC-CHEMICAL

The drift-scale thermal-hydrologic-chemical model is a two-dimensional dual-permeability "chimney" model that extends from the surface to the water table. It includes geologic layering consistent with the flow model. The model is more refined in and around the drift region, where it captures the features of the waste package and invert. It predicts transient water and gas chemistry, mineralogy, porosity, and permeability for 100,000 years. A 50-year ventilation period is simulated, as well as three infiltration scenarios corresponding to the three climate states. The model is validated through predictions and comparisons to the measured gas and water chemistry from the Drift Scale Test.

## 2.4 UNSATURATED ZONE TRANSPORT

There are two distinct unsaturated zone transport modeling approaches: (1) a process model that tests and evaluates various transport processes and mechanisms, and (2) a total system performance assessment (TSPA) particle-tracking model that incorporates the tested transport processes and mechanisms. The process model is used to gain confidence in understanding the impacts of various processes such as matrix diffusion, sorption, colloid filtration, and decay.

It includes advection, dispersion, sorption, matrix diffusion, radioactive decay and daughter products, and colloid transport. The model uses geologic and hydrologic parameters from the flow model and transport parameters from *Unsaturated Zone and Saturated Zone Transport Properties (U0100)* (CRWMS M&O 2001) and *UZ Colloid Transport Model* (CRWMS M&O 2000b). The model consists of two-dimensional and three-dimensional numerical simulations that can efficiently simulate radionuclide transport.

The TSPA transport model uses the FEHM particle-tracking algorithm. It also considers advection, dispersion, matrix diffusion, sorption, and colloidal transport. It uses the flow fields generated from the flow model, so the dual-permeability nature of flow through fractures and matrix is preserved.

Uncertainty in the radionuclide source-term location is implemented by using discretized zones in the repository region. The zones are based on ranges of infiltration (0 to 3, 3 to 10, 10 to 20, 20 to 60, and >60 mm/yr). The release of radionuclides occurs at a random location within one of these five zones depending on the zone in which the release occurs in the engineered barrier system models. Four zones are also defined at the water table, where radionuclide mass is collected for release at a random point in the saturated zone model.

# 3. SUMMARY OF RECENT TEST RESULTS AND OTHER ADDITIONAL INFORMATION

This section summarizes recent results obtained from the different field or laboratory tests that have provided information relevant to enhancing our understanding of the unsaturated zone flow

and transport model. The testing areas that provided this additional information are listed below and discussed in each of the sections that follows.

- Systematic hydrologic characterization
- Cross-Drift bulkhead moisture monitoring
- Alcove 8–Niche 3
- Seepage testing at niches
- Chlorine-36/validation
- Unsaturated zone geochemistry
- Natural analogues
- Busted Butte
- Expected case modeling
- Discrete fracture network modeling.

A schematic of the location from which the additional information was obtained is presented in Figure 1.

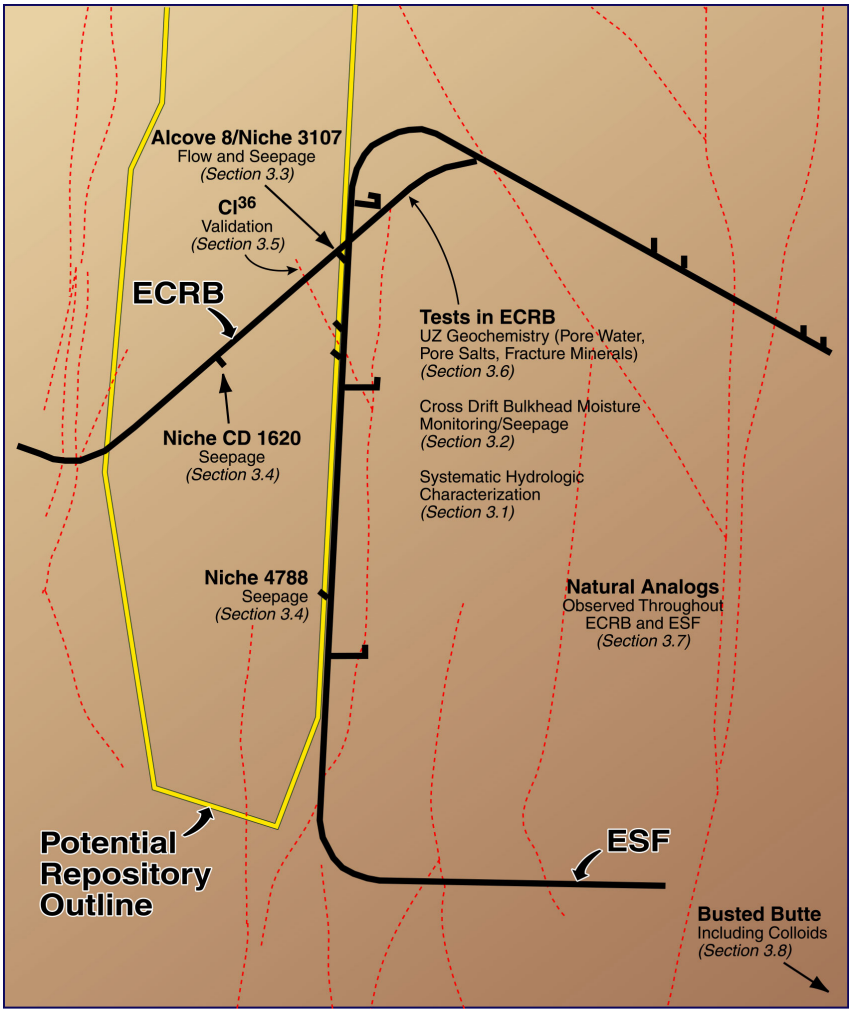


Figure 1. A Schematic of the Location of the Additional Data and Information as Discussed in their Respective Sections

Because of the recent nature of the information provided in this section, much of it is unpublished and, therefore, some source references have been provided where appropriate, but others could not be provided. However, this information is currently documented in the principal investigators' scientific notebooks, if applicable, in accordance with the Project's quality assurance procedure AP-SIII.1Q, *Scientific Notebooks*.

## 3.1 SYSTEMATIC HYDROLOGIC CHARACTERIZATION

### 3.1.1 Introduction

A systematic approach, involving borehole testing at regular intervals along the Enhanced Characterization of the Repository Block (ECRB) Cross-Drift is used to characterize hydrologic attributes within the lower lithophysal unit of the Topopah Spring welded tuff (TSw). The welded tuff in the lower lithophysal unit contains many small fractures (less than 1 m (3.2 ft) in length) interspersed with lithophysal cavities ranging in size from 15 to 100 cm (5.9 to 39.4 in.). Size and spacing of both fractures and lithophysal cavities vary appreciably over an 800 m (2,625 ft) stretch of the Cross-Drift. This indicates that hydrologic characteristics at one particular location may not be representative of the entire unit. Given this possibility, testing at regular intervals would be the optimum approach for acquiring knowledge of the heterogeneous hydrologic characteristics of this unit, in which over 80 percent of the potential repository could reside. This approach complements other hydrologic testing in the ambient testing program, in which test locations are selected either by avoiding or focusing on specific features (such as large fractures, or abundant fractures or cavities). Systematic hydrologic characterization focuses on the hydrologic properties that are important to repository performance. Field measurements include:

1. Air-injection tests that give a measure of fracture permeability

2. Liquid-release tests that determine the ability of the open drift to act as a capillary barrier (diverting water around the drift) as well as the potential of the water to seep into the drift

3. Crosshole gas tracer tests to measure the effective porosity of the rock mass.

The equipment system has been custom-designed for the systematic characterization study based on two criteria: automation and mobility. Field-scale measurements involving liquid flow in unsaturated rock require continuous testing, lasting for weeks to months, whereas the Cross-Drift is open only for eight hours, four days every week. Therefore, the control of test equipment has been fully automated, allowing remote manipulation via computer network when there is no human presence at the field site. All equipment needed for the systematic characterization has been designed as a complete unit to fit on flatbed rail cars. This enables investigators to efficiently transport equipment from one test station to another along the Cross-Drift.

### 3.1.2 Summary of Information Supporting the YMS&ER and YMPSSE

Current knowledge of unsaturated zone flow and transport presented in the YMS&ER (DOE 2001a) and the YMPSSE (DOE 2001b), based on tests at niches in middle nonlithophysal zone of TSw, show that in the potential repository units:

1. Water drainage is expected to be good as a result of the generally high fracture permeability.

2. Open emplacement drifts act as capillary barriers, impeding water from seeping into the drifts and diverting some fraction of the prevailing percolation flux around the drifts.

3. A critical percolation flux (seepage threshold) exists below which no seepage occurs. The distribution of seepage thresholds depends on the hydrologic characteristics and variability of the unit.

4. Ventilation reduces seepage of liquid water. Neglecting ventilation effects in seepage models is conservative.

### 3.1.3 Summary of Recent Test Results and Other Additional Information

At the time of writing for YMS&ER (DOE 2001a) and YMPSSE (DOE 2001b), most of the unsaturated zone flow and transport testing was carried out in the middle nonlithophysal Topopah Spring Tuff in the Exploratory Studies Facility (ESF). The nonlithophysal unit has many well-connected fractures that are longer than 1 m (3.3 ft) in length. Conversely, the lower lithophysal unit, in which systematic testing is currently being carried out, has only small fractures and an abundance of lithophysal cavities. A systematic approach—testing at regular intervals regardless of specific features arising from spatial heterogeneity—has been chosen to perform hydrologic characterization effort. With automatic data collection setup and with water supply and seepage collection equipment mounted on mobile rail flatbeds, the systematic hydrologic characterization can test many borehole zones when tunnel access is readily available. To date, air-permeability and seepage tests were conducted along multiple zones in three 20-m (66-ft) long boreholes, drilled into the crown of the Cross-Drift at a 15° angle from the horizontal with borehole-to-borehole spacing of 30 m (100 ft). The zone length of ~ 2 m (7 ft) or longer were chosen to average over cavity size and fracture length.

The test data to date indicate that small fractures are well connected, giving rise to air-permeability values on the order of $10^{-11}$ $m^2$. The connected fractures probably constitute the main contribution to liquid flow. Figure 2 compares the ranges of variation of permeability data from three zones of a systematic borehole with the borehole data of Niche 5 in lower lithophysal zone, as well as with the site averages (over 7 boreholes) of three niches in the middle nonlithophysal zone of TSw. The lower lithophysal tuff has higher permeability than middle nonlithophysal tuff.

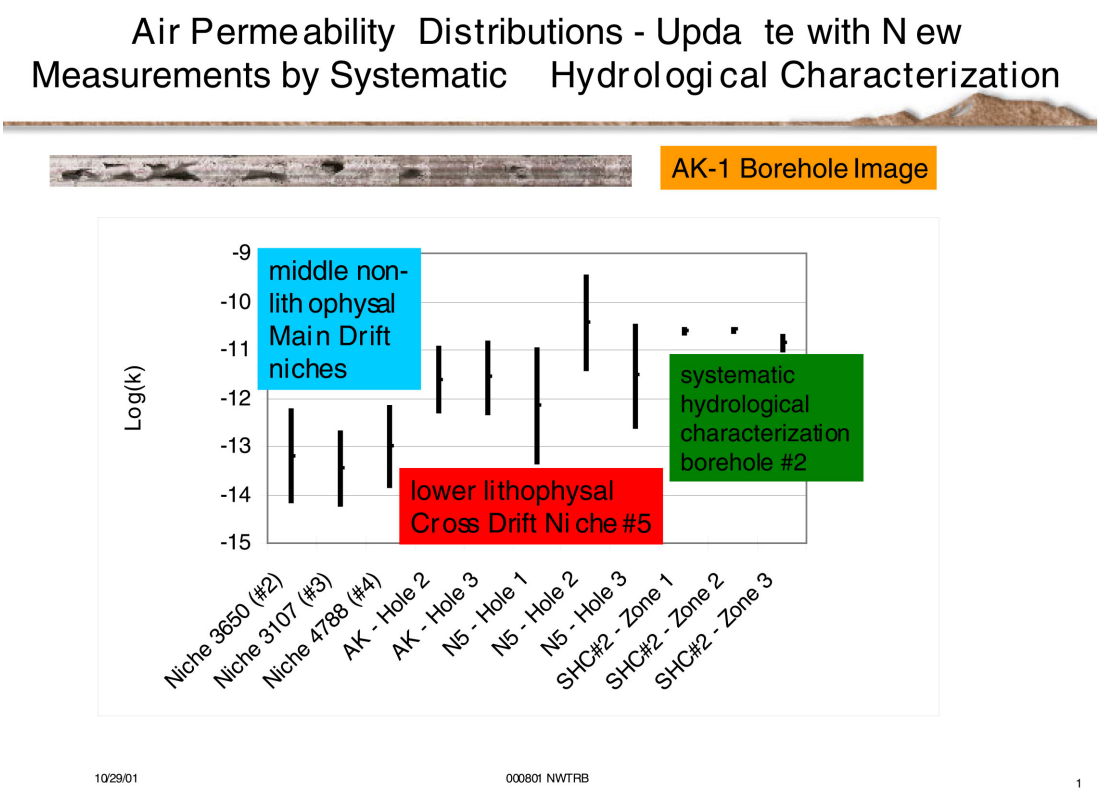


Figure 2. Comparison of Air-Permeability Distributions of Three Zones in Systematic Borehole ECRB-SYBT-LA#1, Five Boreholes at Niche CD 1620 (#5) in Lower Lithophysal Zone, with Site Averages (Over Seven Boreholes) of Three Niches in Middle Nonlithophysal Zone of the Topopah Spring Welded Tuff Unit at Yucca Mountain

Fracture permeability determinations are also being investigated using measurements of radon concentrations. Radon, emitted by the decay of radium in the rocks at Yucca Mountain, has been detected in the tunnel atmosphere of the ESF. Measurements in the ESF underground tunnel atmosphere has shown that radon concentrations are sensitive to ventilation and barometric pressure. These measurements were conducted due to the worker health issues surrounding radon gas; however, a model is being developed to interpret these measurements in terms of large-scale permeability of the rock fractures. The preliminary findings indicate that for large sections of rock, the fracture permeability is on the order of $1 \times 10^{-11}$ $m^2$. These findings are consistent with independent measurements (CRWMS M&O 2000c) of large-scale gas movement through the rock performed using borehole gas pressure measurements.

In the transient process of establishing flow paths, some water imbibes into the low-permeability rock matrix and some seeps into the lithophysal cavities. However, water flow occurs mainly in the fractures, with little participation from the matrix or lithophysal cavities.

Under steady-state conditions, water introduced from one to several meters above the drift flows down toward the drift not in a uniform plume, but along preferential paths. A fraction of the water would miss the drift because of nonuniform flow from fracture heterogeneity, and a fraction of water would be diverted around the drift because of capillary effects. Figure 3

illustrates the evolution of one test sequence of liquid injection and seepage, with transient storage and steady-state seepage development.

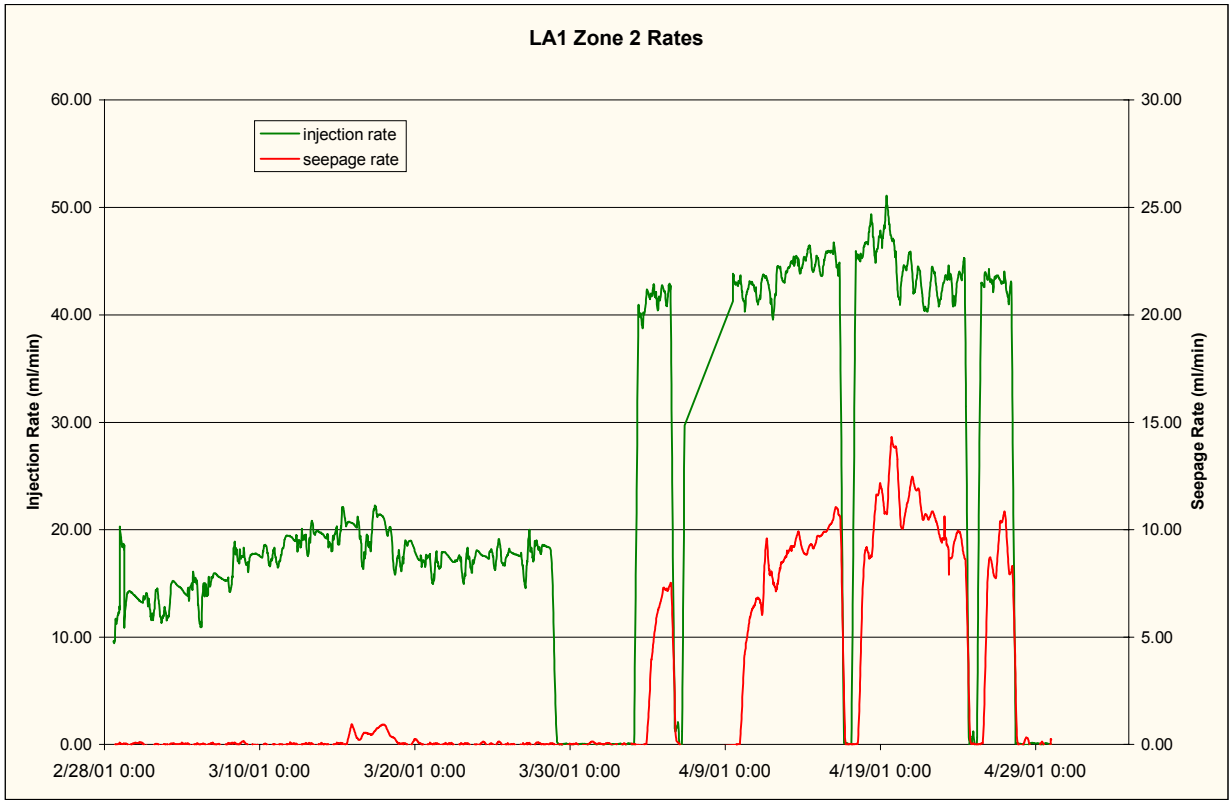


Figure 3. Water Supply Rate and Seepage Rate in ECRB-SYBT-LA#1 Zone 2 for Test Performed on February 28 to April 30, 2001

Relative humidity measurements and open-pan evaporation measurements were incorporated into the systematic-testing equipment system, so that the effects of evaporation are considered in interpreting the seepage data from systematic testing. Upper bounds of seepage loss to evaporation loss were established from open-pan measurements of evaporation rate and from extent of wet area observed on the drift ceiling. The evaporation loss alone cannot explain the difference between water supply rate and seepage rate. The lower lithophysal tuff has the capacity to greatly suppress seepage and seepage diversion occurs. Preliminary results of seepage testing in the TSw lower lithophysal unit suggest that the seepage threshold is about an order of magnitude higher than the seepage threshold value for the TSw middle nonlithophysal unit (BSC 2001a, Figures 4.3.4-4 and 4.3.4-5).

## 3.2 CROSS-DRIFT BULKHEAD MOISTURE MONITORING AND SEEPAGE OBSERVATIONS

### 3.2.1 Introduction

Observations were made in closed drift sections that showed the existence of water, as well as rust spots and organic material (i.e., indicators of the prolonged presence of water). To date, no continuous seepage from the rock into the closed sections of the Cross-Drift has been observed. Saturation and water potential data indicate that the rock is still rewetting. The observed water could have originated from condensation of water vapor, based on available chemical analyses. The water vapor could be derived from pore water or seepage.

To observe potential seepage, ventilation effects have been minimized in the terminal section of the ECRB Cross-Drift with the installation of three bulkheads. The first two bulkheads at Stations 17+63m and 25+03m were installed in the Cross-Drift in June 1999. The influence of heat sources (associated with the tunnel boring machine used in the Cross-Drift excavation in 1997 and 1998) on tunnel conditions was recognized to be a problem, and a third bulkhead (at Station 25+99m) was installed in July 2000. These sections are located in the area of the drift most likely to show seepage under ambient conditions, as predicted by the site-scale unsaturated zone flow model and drift-scale seepage model.

### 3.2.2 Summary of Information Supporting the YMS&ER and YMPSSE

Initial modeling studies of the bulkhead experiment were carried out in 1996 and 1997 to evaluate changes in moisture conditions in the rock surrounding the drift. The rate and extent of rock dryout during the ventilation period and rewetting after installation of the bulkhead were evaluated using the site-scale unsaturated zone flow model. In the calculations for dryout, the extent of drying was found to be less than 10 m (33 ft) within 100 years (Ahlers et al. 1996). For the rewetting period after installation of the bulkhead, the models predicted that the fractures would resaturate within 6 months for the reference case, whereas the matrix would require more than 6 years to completely resaturate (Bodvarsson et al. 1997).

The probability of seepage in the isolated section of the ECRB Cross-Drift was evaluated in fiscal year 2000 using the TSPA seepage-model abstraction. This study assumed that the Cross-Drift had returned to undisturbed moisture conditions in the rock for present-day climate. The seepage results were reported by Stefan Finsterle at the Unsaturated Zone Process Model Report Interactive Review meeting (January 10, 2000). The seepage modeling exercise predicted that there is a 50 percent chance that one or more seeps will occur in the isolated section of the Cross-Drift. Additional seeps are predicted at lower levels of probability; for example, there is a 10 percent chance to see four or more seeps between Cross-Drift Stations 20+00m and 22+00m or two or more seeps between Cross-Drift Stations 24+00m and 25+00m.

### 3.2.3 Summary of Recent Test Results and Other Additional Information

Along the Cross-Drift (before and after the bulkhead installations), humidity, temperature, and barometric pressure have been measured at various stations to provide information on moisture evolution along the Cross-Drift. Additionally, psychrometer measurements of water potential

are being made along the length of boreholes drilled into the drift wall before and between the first and second bulkheads. Visual observation and additional information on the moisture conditions within the nonventilated zone has been obtained during several periods when the bulkhead doors were opened: (1) January 12 to 13, 2000; (2) July 2000 to install the third bulkhead, (3) January 22 to 25, 2001, (4) May 22, 2001, to repair electrical power, and (5) October 1 to approximately November 2001.

During the entries, the entire Cross-Drift was accessible for visual inspection. Wet spots were observed and water samples were collected from small pools of water. The visual observations from the latest entry support the conclusions from early entries that the observed water originates from condensation. For example, water droplets were observed on a painted surface of the drift wall, an impermeable barrier to the rock, as illustrated in Figure 4. Sections of Cross-Drift were observed to be wet enough to discolor the cloth tarps installed in the Cross-Drift for water detection, as illustrated in Figure 5. Both photos were taken in the latest (October 2001) entry.

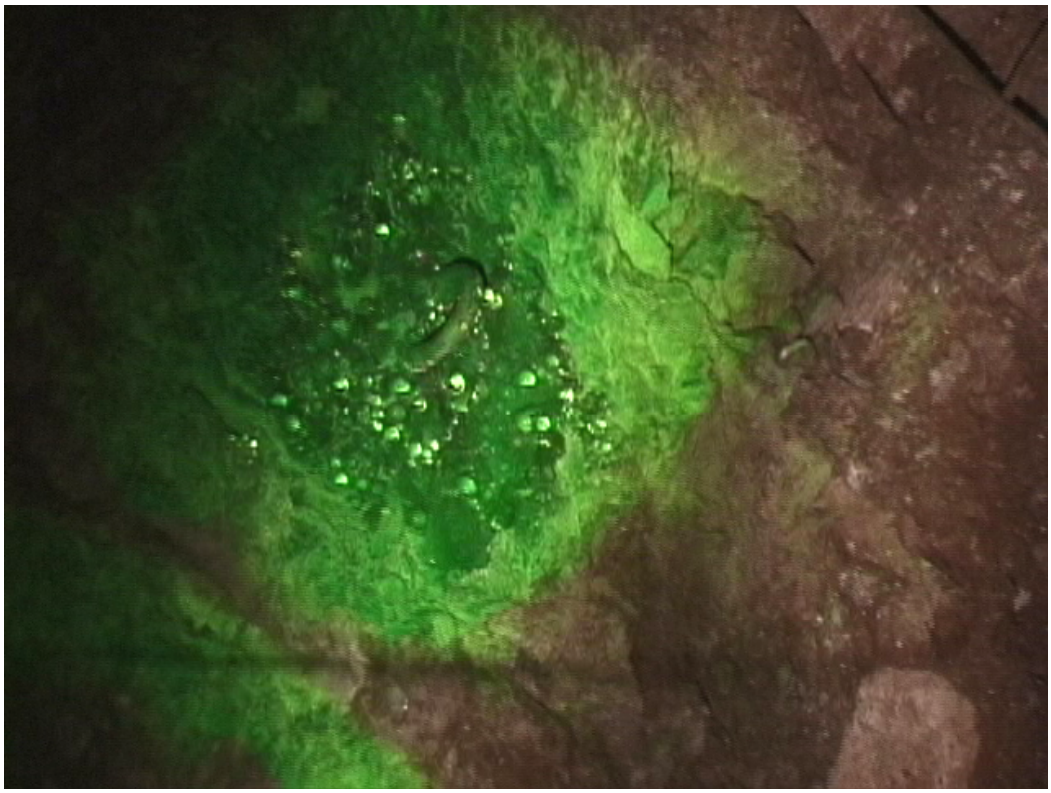

Figure 4. Water Droplets Observed on October 2, 2001 on a Painted Surface (an Impermeable Barrier) with Surrounding Bare Tuff Surfaces Damp but Without Droplet Formation

The water sampled from collection containers in the second entry indicated that the water is low in chloride and silica contents, characteristic of condensate (Figure 6). The water does not have the chemical signature of construction water (that is spiked with about 20 mg/L of lithium bromide). Condensation of water vapor within the isolated portion of the Cross-Drift could result from local temperature variations. The moisture conditions measured by humidity and temperature probes support the presence of drift temperature and moisture variations, as illustrated in Figure 7 and Figure 8.


Figure 5. Discoloration of Tarp for the 6-m Section Before the Third Bulkhead (at ECRB Cross-Drift Station 25+99)

Water-potential measurements along three horizontal boreholes in the Cross-Drift are summarized in Figure 9. The general pattern to the spatial variability within boreholes is that the lower water potentials close to the drift increase rapidly over a distance of 1 to 2 m (3.3 to 6.6 ft) and then remain close to saturation values along the deeper profile. Among the three monitored boreholes, the one located at Station 15+00m has the lowest water potentials close to the drift wall. The borehole at Station 20+00m also has lower water potentials up to a distance of ~1.5 m (4.9 ft) from the borehole collar in September 1999 (prior to the location of the bulkhead doors), which have since increased over a period of 1.5 years. The borehole located furthest into the Cross-Drift at Station 25+00m did not show large drops in water-potential measurements closer to the collar, nor did the borehole show any increases in water potentials following the installation of the bulkhead doors. Figure 9 shows that the rewetting of tuff matrix to its ambient conditions is a slow process.

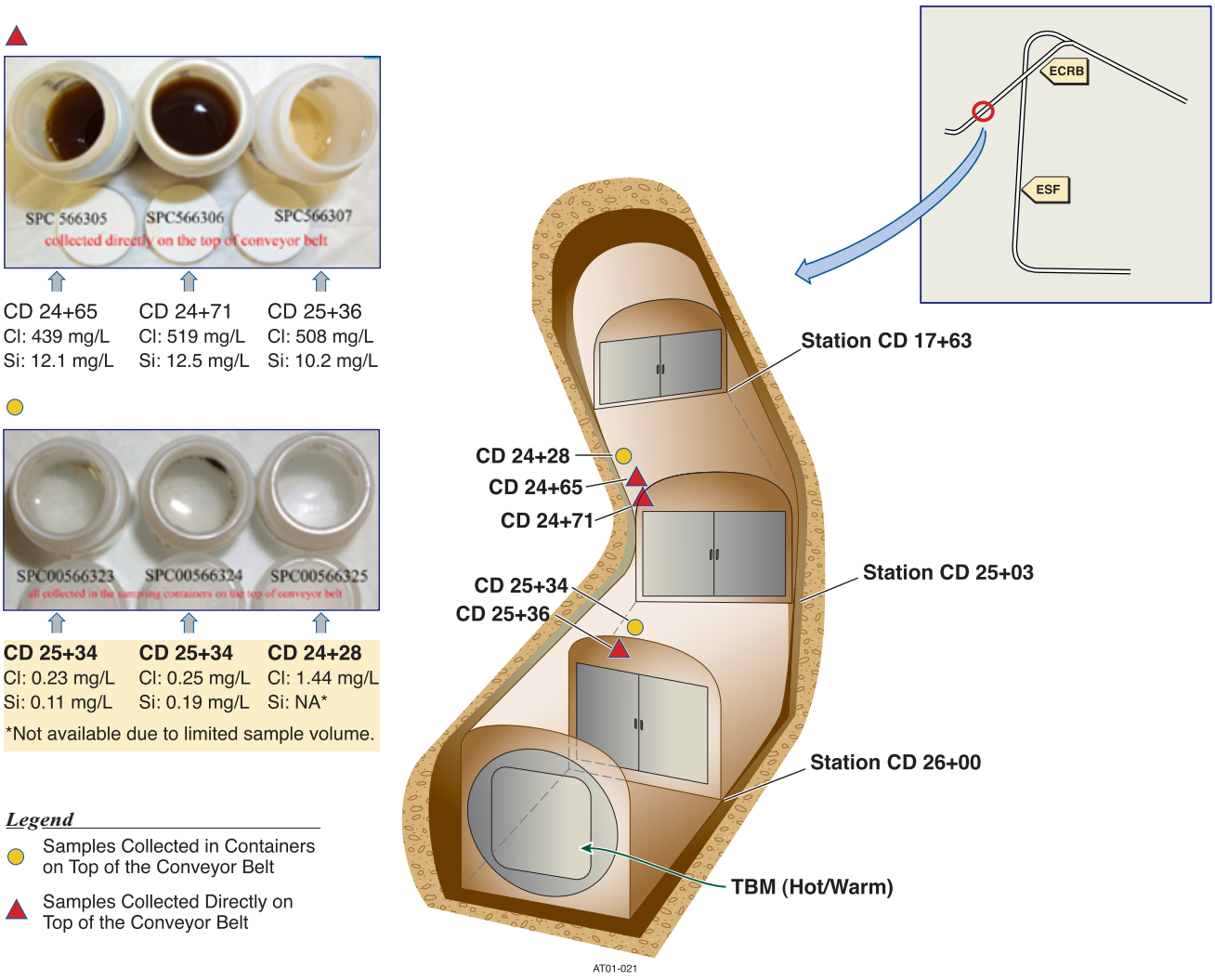


Figure 6. Chemical Analyses of Water Samples Collected on Conveyer Belt and in Containers

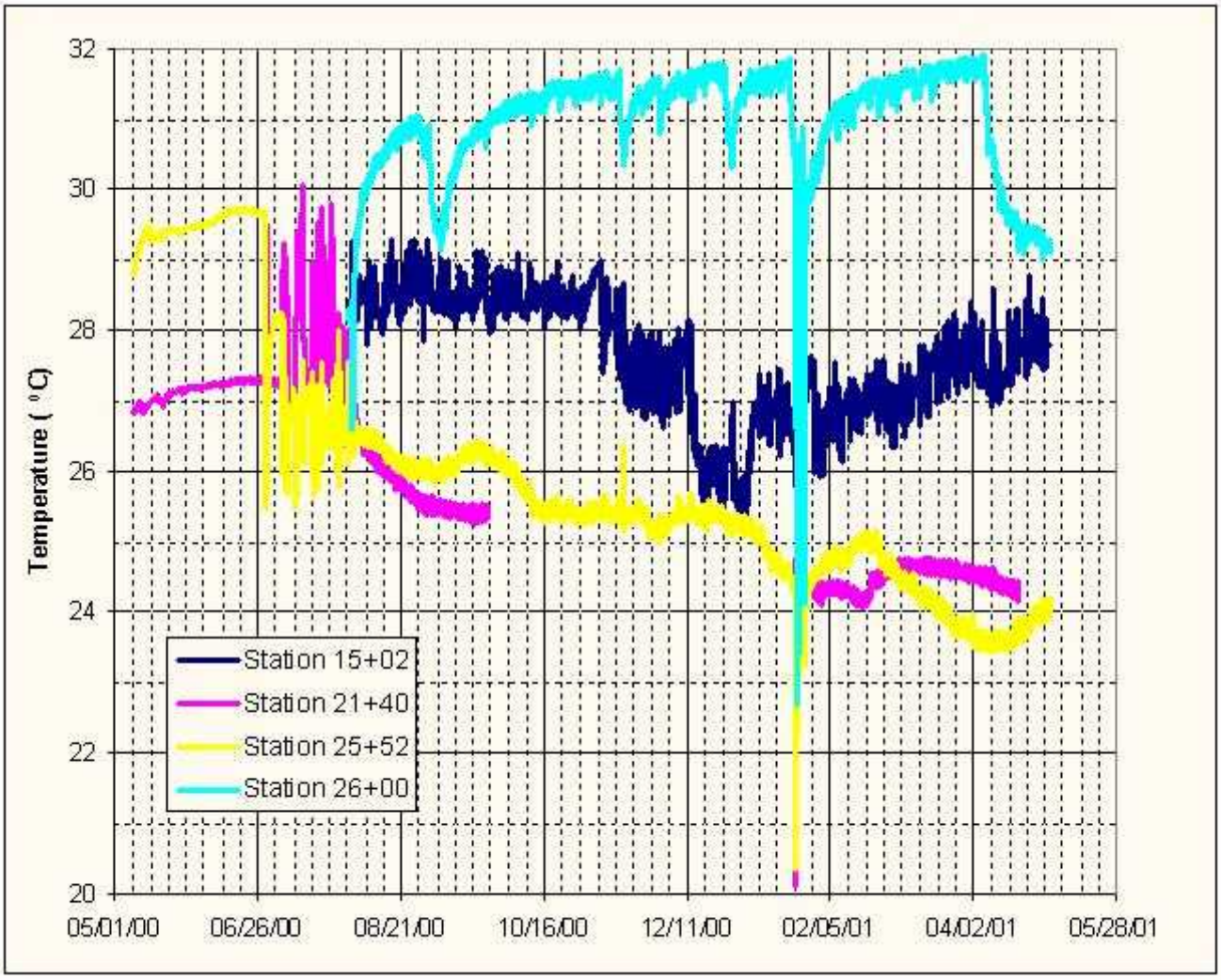


Figure 7. Temperature Measured in the Four Cross-Drift Stations

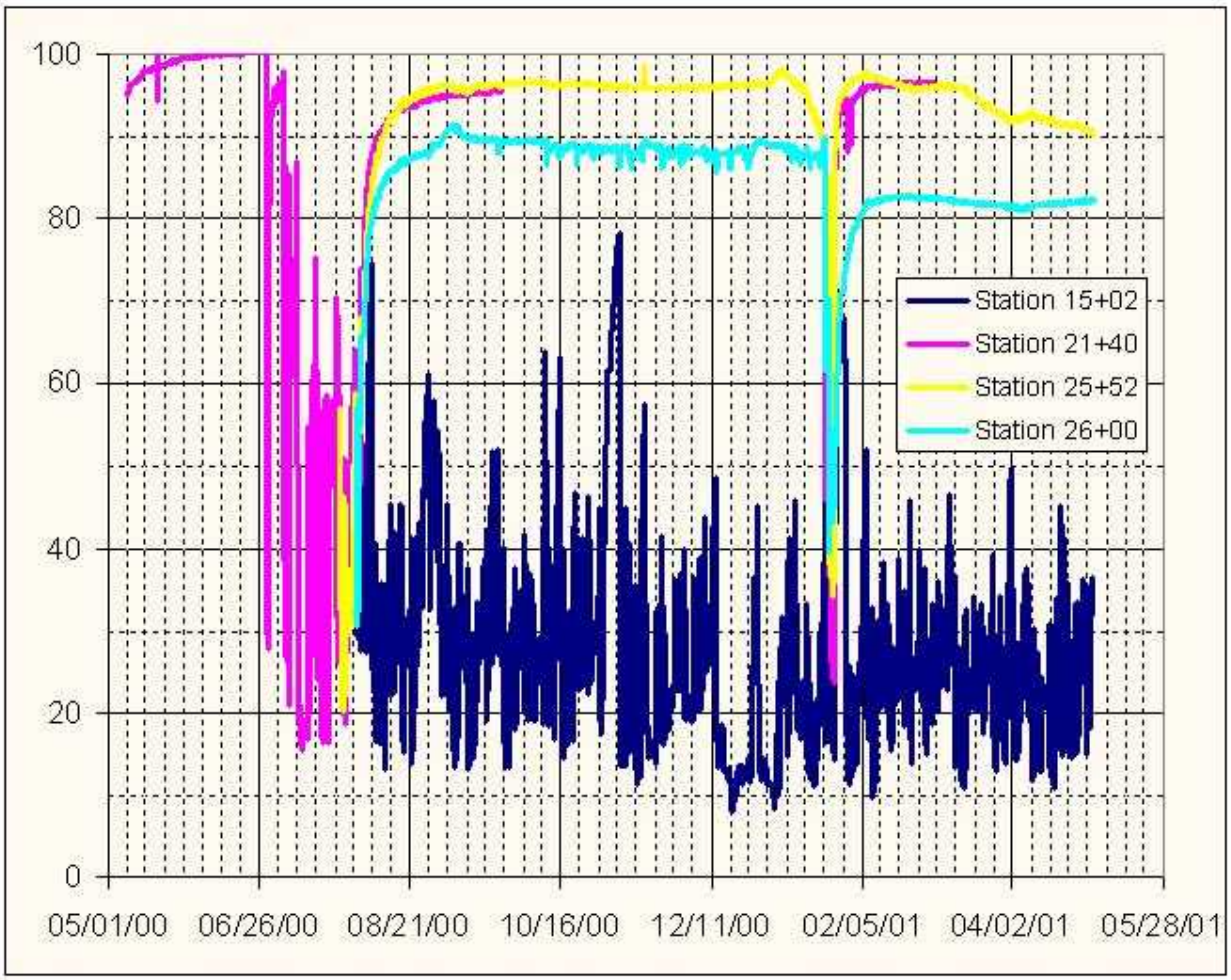


Figure 8. Relative Humidity Measured in the Four Cross-Drift Stations

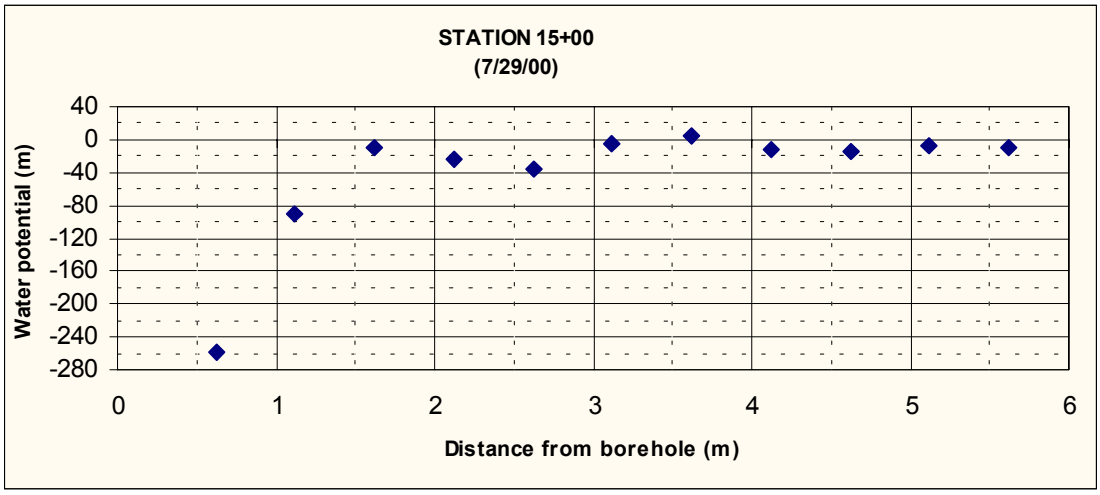


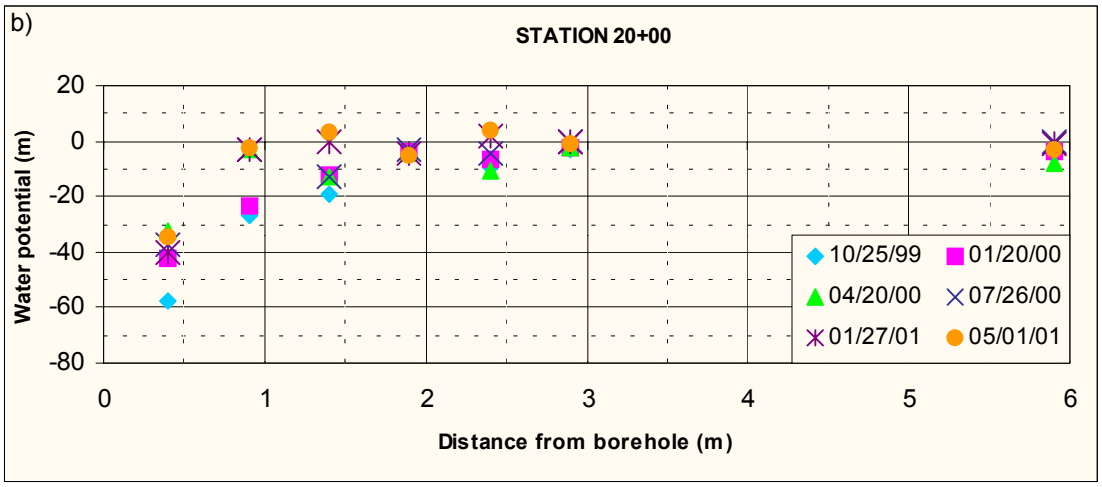


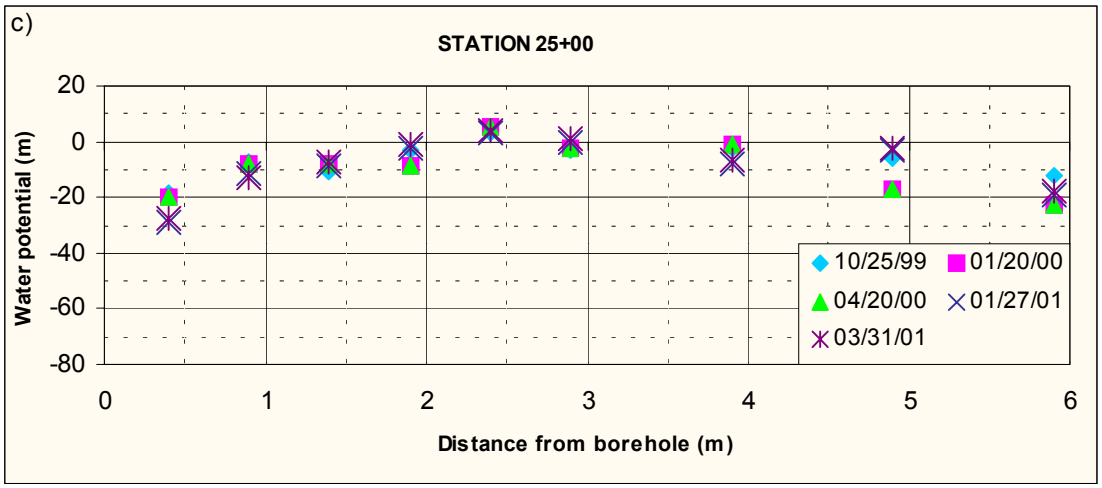


Figure 9. Water Potential Measurements along the Cross-Drift. (a) Station 15+00m before the bulkheads; (b) Station 20+00m; (c) Station 25+00m, both between the first and second bulkhead.

## 3.3 PRELIMINARY OBSERVATIONS FROM THE FAULT TEST AT ALCOVE 8/NICHE 3

### 3.3.1 Introduction

The Alcove 8/Niche 3 test is aimed at determining matrix diffusion, seepage response, and flow within the unsaturated zone at Yucca Mountain. This study represents a new testing program and was not part of the process model as discussed in the YMS&ER (DOE 2001a) and YMPSSE (DOE 2001b). A near-vertical fault that intercepts the formation between Alcove 8 and Niche 3 provides a unique opportunity to evaluate important hydrologic parameters associated with matrix diffusion and fracture-matrix interactions. Tracer mixtures with relatively large and small molecular diffusion coefficients are used to evaluate the importance of matrix diffusion from observations of breakthrough times and the fracture-matrix interfacial area.

Alcove 8 (located at Station 8+00m in the Cross-Drift of the ESF) has been excavated for liquid releases through a fault and a network of fractures. Niche 3 (located at Station 31+07m in the main drift of the ESF) serves as the site for monitoring the wetting-front migration and for collection of seepage originating at Alcove 8. Niche 3 has been instrumented with water-collection trays, and a series of boreholes surrounding the niche has been instrumented with sensors to detect the wetting-front arrival. Additional boreholes have been drilled in Alcove 8 and Niche 3 for geophysical measurements and/or other tests to characterize the plume migration.

Numerical modeling studies have been used for designing the test and are used for the interpretation of data, calibration of rock properties, and validation of numerical approaches used in the unsaturated zone models.

The major test objectives are:

1. Quantification of large-scale (~20 m [66 ft]) infiltration and seepage processes along a fault in the potential repository horizon.

2. Estimation of relations between relative permeability and water potential for unsaturated flow in faults and fracture networks.

3. Evaluation of the importance of matrix diffusion in unsaturated zone transport processes.

### 3.3.2 Summary of Information Supporting the YMS&ER and YMPSSE

As indicated above, this study is a new testing program and no information from this program was available to support the YMS&ER (DOE 2001a) and YMPSSE (DOE 2001b).

### 3.3.3 Summary of Recent Test Results and Other Additional Information

The first phase of the test began on March 6, 2001, when water was released along the fault in Alcove 8. This release has continued largely uninterrupted under ponded conditions (2 cm [0.8 in.] of water head). Water was first detected within the monitoring boreholes located

immediately above the niche and then observed as seeps in Niche 3. As cumulative seepage to the niche increased, measurements of seepage rates at localized zones suggest steady-state conditions.

As of May 31, 2001, 15,404 L (4,069.3 gal) of water had been applied to the entire trench over a period of 2,102 hours of infiltration (87.5 days). The data in Figure 10 suggest that until around 4/20/01, the intake rates fluctuated significantly along the fault, after which the rates reached quasi-steady-state conditions ranging from about 25 L (6.6 gal) per day to about 80 L (21 gal) per day.

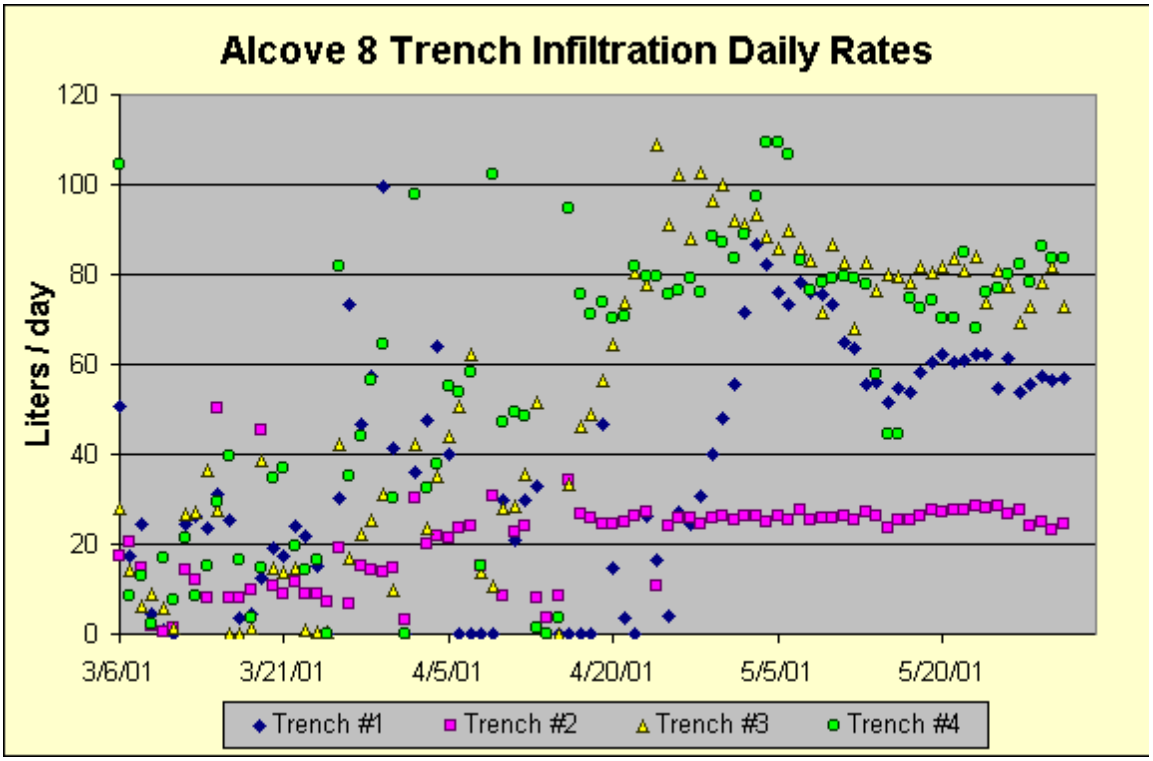


Figure 10. Infiltration Rates Along a Fault through Four Trenches in Alcove 8

The advancing edge of the wetting front was detected 1.9 m (6.2 ft) from the collar of borehole 10 on April 9, 2001, 34 days after the start of liquid release along the fault in Alcove 8 (Figure 11). This plume was observed to extend between 1.65 and 2.40 m (5.41 and 7.87 ft) from the collar in borehole 10 over the next seven days.

Water was first observed along the exposed fault at Niche 3 on April 10, 2001. Over the next few weeks, the number of seeps along the fault in Niche 3 gradually increased. By July 18, 2001, ~1,400 L (370 gal) of water had been collected from seeps into Niche 3 (Figure 12). The seepage rate from a single seep location suggests that following first measurable seepage, seepage rates climbed to near steady values in the next four weeks (Figure 12).

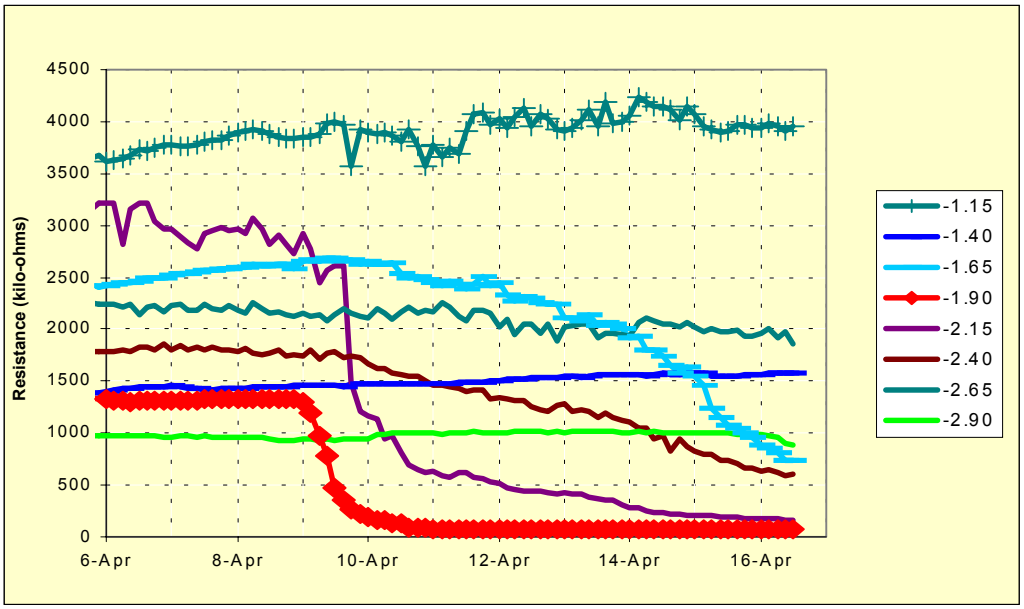


Figure 11. Wetting-Front Arrival Detected in Borehole 10 in Niche 3. Legend indicates the location of measurement (in meters) from borehole collar.

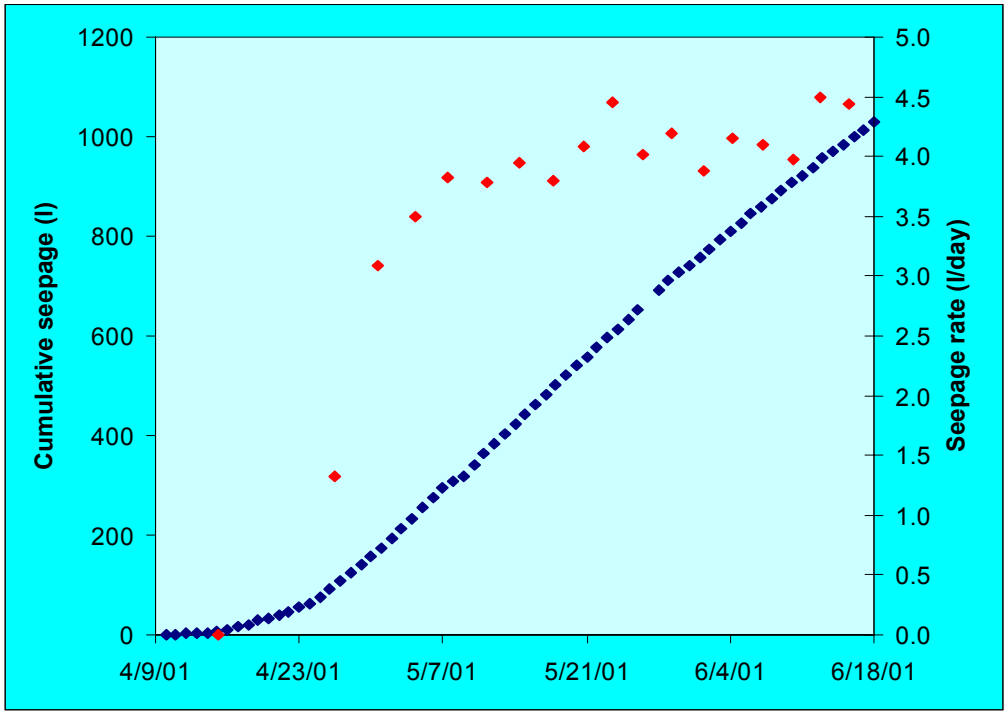


NOTE: Blue diamonds represent cumulative seepage, red diamonds represent seepage rate measurements.

Figure 12. Cumulative Seepage from all Collection Trays in Niche 3 and the Seepage Rate Observed along a Section of Fault in Niche 3 (as measured in Tray U3-B4)

## 3.4 SEEPAGE TESTING AT NICHES

### 3.4.1 Introduction

Four niches are located along the ESF main drift and one niche is located in the Cross-Drift. The niches along the ESF main drift were excavated in the middle nonlithophysal zone of the TSw. Cross-Drift Niche 5 is located at construction Station 16+20m of the Cross-Drift. The niche was constructed in the lower lithophysal zone of the TSw in May 2000.

### 3.4.2 Summary of Information Supporting the YMS&ER and YMPSSE

Specific seepage-related issues (such as flow focusing, rock bolts, drift degradation, and the impact of thermal, chemical, and mechanical effects on seepage) are presented in detail in Volume 1, Sections 4.2.1 to 4.2.6 of *FY01 Supplemental Science and Performance Analyses* (BSC 2001a). A summary of the key model processes is presented below.

**Spatial and Temporal Flow Focusing**—Flux and spatial distribution of downward percolating water is one of the most important factors affecting seepage rates and seep locations. Water movement is controlled by net infiltration at the surface and subsequent multiscale moisture redistribution. Hydrostratigraphic units and features govern large-scale flow patterns, and thus lead to a redistribution of infiltration and percolation fluxes. On an intermediate scale, flow through the fracture network may be focused (funneling effect) or dispersed (bifurcation). This leads to zones of locally higher percolation fluxes and areas of reduced water flow between them. Finally, heterogeneity and flow instabilities within individual fractures lead to small-scale flow channels (rivulets or fingers). In addition to spatial flow focusing, episodic events may lead to temporally increased percolation fluxes, followed by periods of reduced percolation.

**Capillary-Barrier Effect**—Under unsaturated conditions, the rate of water dripping into the opening is expected to be less than the downward percolation rate because the cavity acts as a capillary barrier. If percolating water encounters the cavity, the relatively strong capillary forces in the geologic formation retain the water, preventing it from seeping into the drift. Water accumulates at the drift ceiling, where the increase in saturation leads to capillary pressures that are locally less negative than in the surrounding rock, allowing water to be diverted around the drift. If the lateral hydraulic conductivity is insufficient to divert all the water, seepage is initiated.

**Excavation-Disturbed Zone**—The properties of the fractured rock in the immediate vicinity of the drift wall control the capillary-barrier effect, which occurs within a relatively small region around the opening. The thickness of this boundary layer is approximately given by the height to which water rises on account of capillarity, and it is likely to be smaller than the extent of the zone affected by excavation-induced stress redistribution and related rock deformations.

**Drift Geometry and Drift Surface Effects**—The geometry (i.e., the shape and size) of the emplacement drift determines the likelihood of encountering seeps and the ease with which water can be diverted around the opening. The geometry of drift-wall roughness and the characteristics of the drift surface (e.g., wettability, microroughness, dust, coating) partially control local water accumulation, droplet formation, the potential for film flow along the drift

wall, and, eventually, dripping locations. The frequency, location, size, and geometry of breakouts and partial drift collapse affect the integrity of the capillary barrier.

**Ventilation and Evaporation-Condensation Effects**—The drift temperature, drift humidity, and regulation of temperature and humidity in the drift by ventilation determine evaporation and condensation effects. Evaporation at the drift wall generally reduces drop formation and dripping, and creates a dryout zone around the drift. If relative humidity in the drift is kept below 100 percent by ventilation, then seepage of water is reduced or completely suppressed. However, local differences or temporal changes in drift temperature may lead to condensation of vapor, causing droplet formation at the drift wall and other surfaces within the drift. Accumulation of condensate can lead to dripping.

**Thermal Effects and Coupled Processes**—Repository heat may impact seepage through coupled thermal-hydrologic-chemical-mechanical effects on rock properties or through the redistribution of water around the drifts and the development of a vaporization barrier.

### 3.4.3 Summary of Recent Test Results and Other Additional Information

The seepage tests were conducted along four niches along the ESF main drift to estimate the seepage threshold for middle nonlithophysal zone of TSw. Seepage threshold is the flux below which no seepage occurs. The tests were conducted by series of liquid release tests with decreasing flow rates until no water is observed to seep into the niche space. The results of data analyses for short duration tests at Niche 2 (Station 36+50) and long-term tests at Niche 4 (Station 47+88) are illustrated in Figure 13. The long-term tests capture the steady state conditions better and minimize the problems with water storage. The analyses of the long-term tests were completed in 2001. The classical Phillips analytic solution of capillary barrier was used to estimate the capillarity strength parameter $\alpha^{-1}$ in Figure 13.

The relative humidity and temperature of the air within Niche 4 were monitored up through early June 2001. Monitoring took place with the bulkhead doors at the entrance to the niche closed and sealed. Examples of niche conditions and long-term seepage tests are illustrated in Figures 14 and 15.

As shown in Figure 2 in Section 3.1, boreholes at Niche CD 1620 (Niche 5) in lower lithophysal zone have higher air-permeability than values of niches in middle nonlithophysal zone of TSw. The relative changes in permeability before and after niche excavation are smaller in lower lithophysal zone than in middle nonlithophysal zone. Initial seepage testing at Cross-Drift Niche 1620 (Niche 5) was begun in February 2001, but was halted in April to allow for the construction of two slots within the niche. The arrival of the wetting front at the slot can demonstrate that water is diverted by the drift. If the slot can capture all the diverted water, we can use water balance calculations to better quantify the diverted flow field. No seepage or wetting was observed during the short duration of this test. Construction activities were terminated after creating a 2 to 3 m (6.6 to 10 m) long irregular-shaped excavation in the left wall of the niche.

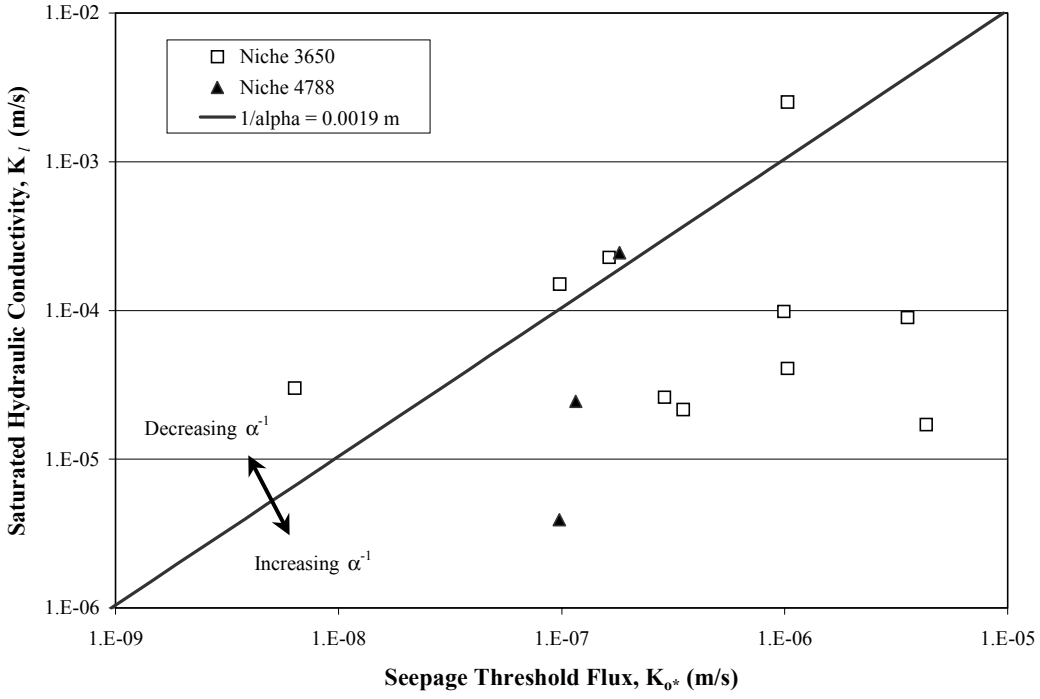


Figure 13. Seepage Threshold Fluxes Determined by Seepage Tests at Middle Nonlithophysal Zone of Topopah Spring Welded Unit

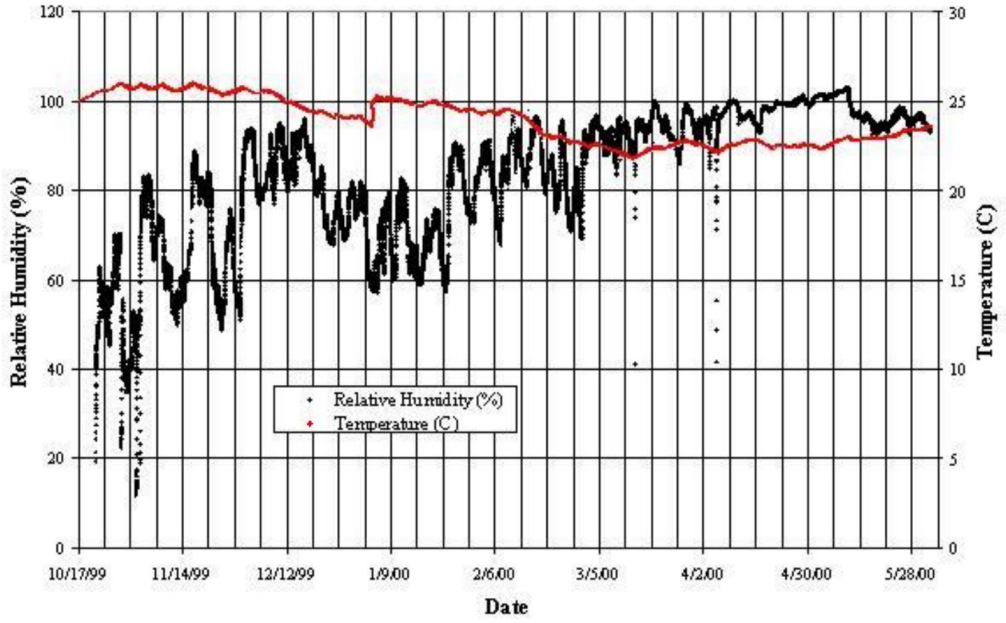


Figure 14. Relative Humidity and Temperature Inside Niche 4788 (Niche 4)

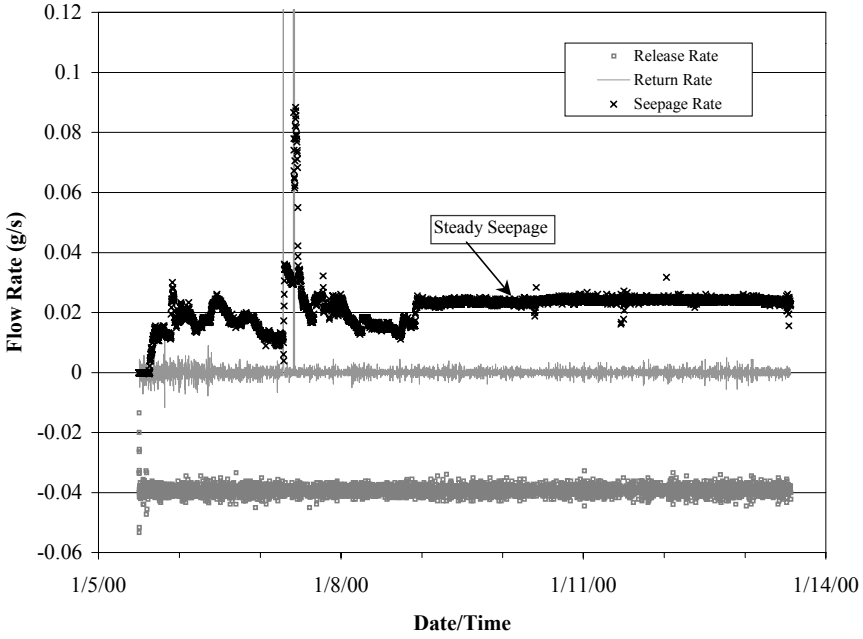


Figure 15. Stablized Flow Rates Observed During Test #1 1-5-00 Conducted on Test Interval UR at Niche 4788 (Niche 4)

The barometric pressure, temperature, and relative humidity of the air within the Niche CD 1620 (Niche 5) were measured from July through August 2001. In addition, the rate that water evaporated from a free surface was measured. Monitoring took place with the bulkhead doors at the entrance to the niche closed and sealed.

## 3.5 CHLORINE-36 AND TRITIUM

### 3.5.1 Introduction

As part of the chlorine-36 validation study, low-level tritium measurements of pore water distilled from unsaturated zone core samples from the ESF at Yucca Mountain are being used to identify the presence of fast pathways. These pathways allow percolation of young water to the potential repository horizon. Much of the tritium data have been collected at locations similar locations to where samples have been collected for chlorine-36 analysis in an effort to obtain corroborating evidence for the interpreted presence of numerous fast paths within the Sundance and Drill Hole Wash Faults.

### 3.5.2 Summary of Information Supporting the YMS&ER and YMPSSE

The YMS&ER (DOE 2001a) mentions the ongoing effort to validate chlorine-36 measurements in the ESF. It discusses the progress made in attempting to develop a standard leaching technique to maximize the yield of meteoric chloride and minimize the yield of rock chloride. The U.S. Geological Survey is currently conducting the leaching of validation core from the ESF, and leachates are being distributed to both Lawrence Livermore National Laboratory and Los Alamos National Laboratory for chlorine-36 analyses. Currently, no additional analyses are available. Tritium analyses of perched water and water extracted from core are mentioned at several places in the YMS&ER. These existing data are generally interpreted to indicate limited fast pathways through the unsaturated zone.

### 3.5.3 Summary of Recent Test Results and Other Additional Information

Natural tritium, with a half-life of 12.43 years, is produced in the atmosphere by neutron bombardment and enters the hydrologic system as precipitation. Estimates of tritium concentrations in precipitation near Yucca Mountain prior to atmospheric testing of nuclear weapons (early 1950s) vary from 5 to 8 tritium units. After weapons testing began, tritium concentrations in precipitation reached thousands of tritium units. Water isolated from the atmosphere in the early 1950s with an initial tritium concentration of 8 tritium units would presently contain less than 1 tritium unit of tritium. Therefore, water with tritium in excess of 1 tritium unit must contain some component of water that infiltrated the site within the last 50 years.

Figure 16 illustrates the sample locations in the ESF. Tritium analyses from 8 samples in Alcove 2 and 18 samples along the north ramp indicate detectable post-weapons-testing tritium occurs only within the Tiva Canyon Tuff at shallow depth in the Bow Ridge fault. No tritium has yet been detected deeper in the unsaturated zone system or lower stratigraphically within the nonwelded units of the Paintbrush Tuff or within the underlying Topopah Spring Tuff along the north ramp. Tritium analyses of 42 samples of pore waters obtained along the Sundance fault and 26 pore-water samples from the Ghost Dance fault within the Topopah Spring Tuff in the main drift of the ESF, indicate that only five contained at least 1 tritium units of tritium. One of the five samples exceeding 1 tritium units came from the Sundance fault, while the other four came from the Ghost Dance fault (one in the northern access drift and three in the southern access drift). This indicates that although fast percolation of young water into the Topopah Spring Tuff does occur along faults, it appears to be extremely isolated in the northern part of the ESF. Along the south ramp of the ESF where the Paintbrush Tuff nonwelded units are offset by numerous faults, 14 of 24 samples contained tritium concentrations greater than 1 tritium units with several samples having concentrations in excess of 10 tritium units. This indicates that fast percolation through the Paintbrush Tuff nonwelded units to the Topopah Spring Tuff is common in the southern part of the ESF.

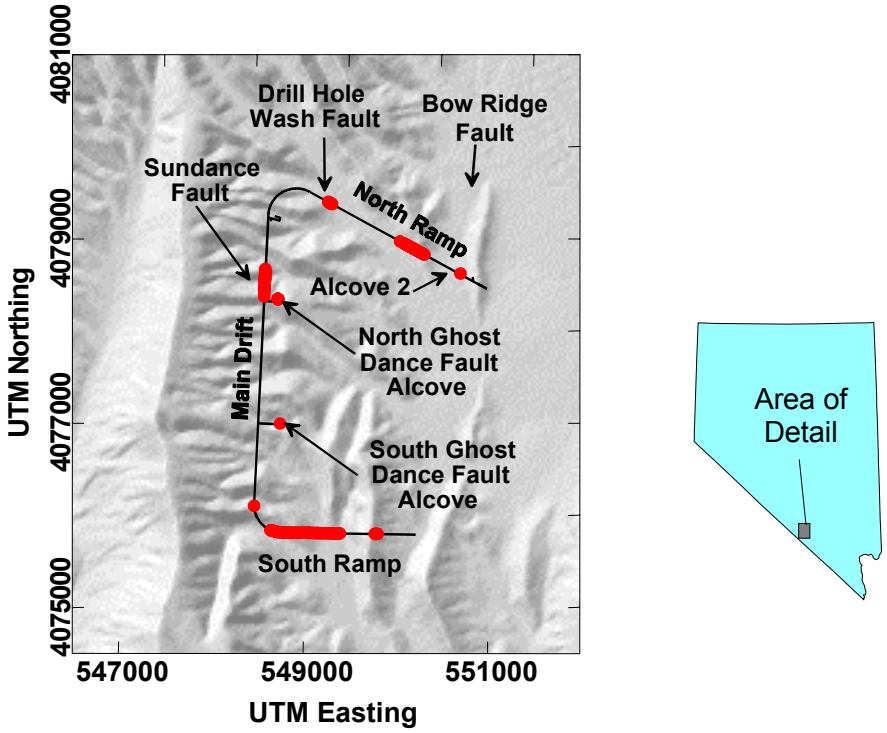


Figure 16. Map of the ESF Showing Sample Locations

## 3.6 UNSATURATED ZONE GEOCHEMISTRY

### 3.6.1 Calcite Abundances

#### 3.6.1.1 Introduction

Geochemical data and interpretations of fracture minerals at Yucca Mountain provide important means of testing the unsaturated zone flow model. Additional work not captured in the current YMS&ER (DOE 2001a) is discussed below.

#### 3.6.1.2 Summary of Information Supporting the YMS&ER and YMPSSE

Within the unsaturated zone at Yucca Mountain, secondary calcite precipitates from films of water percolating downward through the fracture network (Paces et al. 2001). Abundances of calcite within the rock mass are therefore related to relative amounts of percolation flux that may vary both laterally and vertically within the unsaturated zone. Calcite abundances measured in borehole USW WT-24 have been used as a tool for testing the reactive transport model of unsaturated zone flow involving infiltration rate, water and gas compositions, and reactive surface area (DOE 2001a, Section 4.2.1.3.1.5). Simulations of calcite deposition using the model and a range of infiltration rates between 2 mm/yr to 20 mm/yr (0.08 to 0.8 in/yr) are consistent with the wide range of calcite abundances measured in the potential repository units of the TSw from WT-24 borehole cuttings (DOE 2001a, Figure 4-14b). An infiltration rate of approximately

6 mm/yr (0.2 in/yr) was quoted as a value that could account for the average abundance of measured calcite (2,669 µg/g).

### 3.6.1.3 Summary of Recent Test Results and Other Additional Information

The calcite-abundance profile determined for USW SD-6 cuttings (Figure 17) shows substantial differences from the USW WT-24 profile, especially in the units below the PTn. Both profiles generally show decreasing calcite abundances through the TCw into the PTn. In the WT-24 profile, large amounts of calcite are present in the upper lithophysal (Tptpul) unit, and especially in the middle nonlithophysal (Tptpmn) and lower lithophysal (Tptpll) units (Table 1). In contrast, the SD-6 profile contains the largest TSw calcite abundances in the Tptpul, with substantially smaller abundances in the underlying Tptpmn and Tptpll (Table 1 and Figure 17). Although the overall average calcite abundances of all three units is within a factor of 2 between the two boreholes, average abundances for the Tptpmn and Tptpll in the SD-6 cuttings are about 4 times lower than those in WT-24 cuttings.

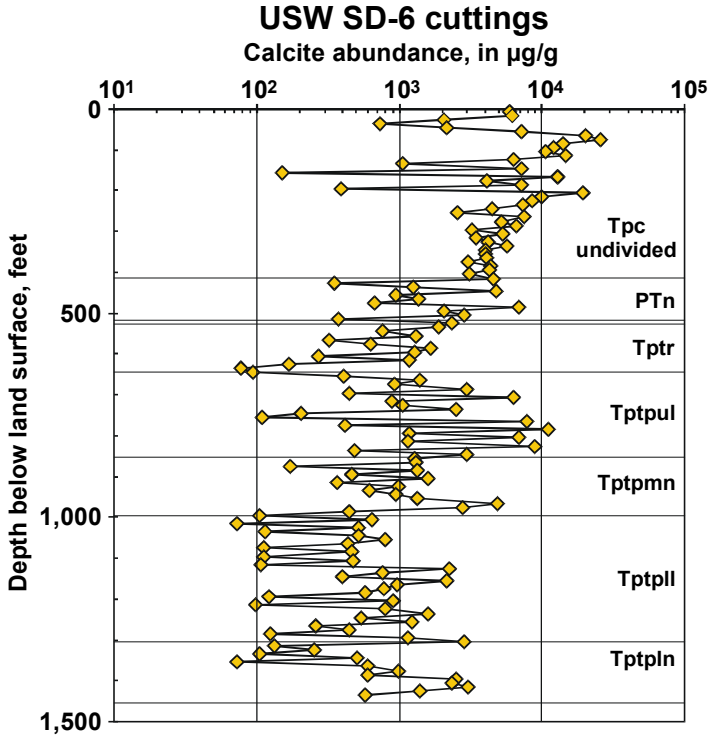


Figure 17. The Calcite-Abundance Profile Determined for USW SD-6 Cuttings

Table 1. Average Calcite Abundances in the SD-6 vs. WT-24 Cuttings

| Stratigraphic Interval | Calcite abundances, in µg/g | |
|---|---|---|
| | WT-24 | SD-6 |
| Average Tptpul to Tptpll | 2,669 | 1,482 |
| Std Dev | 3,543 | 2,076 |
| Max | 18,132 | 11,140 |
| Min | 33 | 73 |
| Average Tptpul | 1,522 | 2,912 |
| Std Dev | 2,890 | 3,362 |
| Max | 14,641 | 11,140 |
| Min | 33 | 109 |
| Average Tptpmn to Tptpll | 3,204 | 847 |
| Std Dev | 3,705 | 875 |
| Max | 18,132 | 4,920 |
| Min | 184 | 73 |

### 3.6.2 Estimates of Seepage from Calcite

#### 3.6.2.1 Introduction

Secondary calcite and silica coatings present on fracture footwalls and lithophysae floors in the welded Topopah Spring Tuff formed from unsaturated zone percolation that seeped into open spaces within the rock mass over the past 13 million years. Because secondary minerals are sporadically distributed in only a small percentage of all lithophysal cavities, matrix flow cannot provide an important seepage component. Instead, fracture flow is considered to be the dominant source of seepage into these cavities. The method used to estimate the volumes of seepage is based on the observation that the ratio of water to calcite is approximately constant during precipitation of calcite from calcite-saturated or over-saturated solutions. The water:calcite volume ratio is approximately $10^5$, with an estimated error of a factor of 10 (Marshall et al. 2000). In other words, for each cubic centimeter of calcite at a given site, $10^5$ $cm^3$ or 0.1 $m^3$ of water passed through that site. This assumes that all water is calcite-saturated and no significant dissolution of calcite has occurred. From extensive geochronologic data on the coatings, it is estimated that most coatings started forming early in the history of the Topopah Spring Tuff and formed at a fairly constant rate up to the present time (Paces et al. 2001). Additionally, isotopic data indicate that, in general, calcite was precipitated from water that interacted extensively with the overlying nonwelded tuffs.

#### 3.6.2.2 Summary of Information Supporting the YMS&ER and YMPSSE

Section 4.2.1.2.11 of YMS&ER (DOE 2001a) briefly mentions that calcite and opal are analyzed to evaluate flow in fractures and seepage into cavities over millions of years. However, the only model presented is one that relates percolation flux to calcite abundances in borehole

USW WT-24 (DOE 2001a, Figure 4-14). Uncertainties in geochemical-model estimates of calcite precipitation are discussed in Section 4.2.1.3.5 of the YMS&ER (DOE 2001a).

#### 3.6.2.3 Summary of Recent Test Results and Other Additional Information

Direct estimates of amounts of past water seepage required to form calcite at a given site have been made (Marshall et al. 2000). These estimates are the result of both simplified geochemical models and published data on both laboratory experiments and other natural calcite occurrences in unsaturated zones. Because the present-day amounts of calcite at a given site are a minimum estimate of what could have been deposited originally, these estimates of past seepage could be viewed as minimum amounts. There are also uncertainties in the estimates because of the episodicity of seepage in both time and space. However, from extensive studies of the calcite and opal coatings (Paces et al. 2001), it is apparent that dissolution of pre-existing calcite is not a common feature, and most coatings display a fairly complete growth history suggesting that seepage locations are constant through time. Calculation of seepage rates is based on a total calcite accumulation time of $10^7$ years. Calculation of the seepage fraction (fraction of waste packages contacted by seepage) is based on geometric extrapolation of detailed line surveys conducted in the ESF, which for the calcite data indicates a value of about 0.5. This simplified model does not take into account the fact that the seepage potential increases with cavity size in a nonlinear fashion. The drift geometry and its impact on seepage are also neglected, i.e., the estimate for seep flow rates based on the calcite data can only provide a lower bound for seepage into potential repository drifts. The seepage estimate from the calcite data indicate a value of about $1.5 \times 10^{-3}$ $m^3$/yr over a 5-m (16-ft) section of the waste emplacement drift. As expected, this seepage rate is substantially lower than predicted in the TSPA model at the same seepage fraction (Wilson and Ho 2001). Therefore, the independent estimate for seepage from calcite data is consistent with TSPA seepage predictions given that (1) the TSPA model is a conservative predictor of seepage (i.e., favors higher seepage where uncertainty is not specifically quantified) and (2) the calcite approach can only provide a lower bound for seepage into potential waste emplacement drifts.

Strontium isotope measurements performed on both calcite and pore-water salts indicate that calcite deposited within the Topopah Spring Tuff was precipitated from water that interacted extensively with the overlying units of the PTn (Marshall and Futa 2001). This information is consistent with the overall YMS&ER discussion, but provides a more convincing argument for the lack of widespread fast paths.

### 3.6.3 Pore-Water Geochemistry

#### 3.6.3.1 Introduction

Approximately 85 percent to 90 percent of water stored in the rock mass above the potential repository level is contained within the densely welded units of the Tiva Canyon Tuff and the Topopah Spring Tuff under the present partial saturation conditions. The remainder is contained in the nonwelded units, particularly those composing the Paintbrush unit (PTn). An estimate of the water budget for the unsaturated-zone rock mass above the level of the emplacement drifts is given in Table 2.

Table 2. Estimated Water Budget for the Unsaturated-Zone Rock Mass above the Level of the Emplacement Drifts

| Lithostratigraphic Unit | Thickness (ft) | $H_2O$ (%) | Saturation (%) | Dist. $H_2O$ (%) |
|---|---|---|---|---|
| TCw | 213 | 5.52 | 75.8 | 11.4 |
| PTn | 85 | 16.33 | 51.6 | 13.5 |
| TSw | 954 | 8.11 | 78.2 | 75.1 |

The water content and saturation figures are averages for analyses of core from SD-7, -9, and -12. The thickness of each lithostratigraphic unit is for SD-12 and is assumed to be representative of the rock mass above the repository level.

### 3.6.3.2 Summary of Information Supporting the YMS&ER and YMPSSE

Discussions of pore-water composition in the YMS&ER (DOE 2001a) are based on analyses that were available for water extracted by uniaxial compression of samples from the nonwelded units, particularly the PTn. Since the YMS&ER (DOE 2001a) was prepared, the U.S. Geological Survey has been extracting (through use of an ultracentrifuge technique) and analyzing water from the lower porosity, densely welded, crystal-poor units of the Topopah Spring Tuff, using core from the Cross-Drift.

In the YMS&ER, the relatively large concentrations of dissolved solids in pore water were taken to indicate limited percolation flux through the rock matrix. At the same time, the chlorine concentrations in pore water were used to conduct chlorine mass-balance calculations for determining the spatial distribution of flux below the PTn. The YMS&ER also recognizes the need to understand the compositional evolution of water downward through the rock mass and the extent of interaction between fracture and matrix water in the densely welded units. The pore water will be mobilized because of the thermal load of a potential repository, and baseline analyses are required to predict the composition modification of the mobilized water, including its ability to dissolve and precipitate secondary minerals.

### 3.6.3.3 Summary of Recent Test Results and Other Additional Information

The U.S. Geological Survey has completed extraction and chemical analyses of 13 pore-water samples from Cross-Drift core at Stations 400, 500, 600, 750, 850, 900, 1,000, 2,000, and 2,150 m. Water is extracted by ultracentrifugation because the compressive strength of the densely welded rocks is too large to allow collapse of the pores and expulsion of contained water by uniaxial compression. Cations, including trace elements, were determined by inductively coupled plasma mass spectrometry, and anions were determined by ion chromatography—except bicarbonate, which was determined by titration. Like water extracted from nonwelded units, the content of total dissolved solids is larger than that of perched water or water in the saturated zone beneath Yucca Mountain.

The new pore-water analyses are summarized in Figure 18, where mean values for the 13 samples are plotted against representative values for borehole UE-25 J-13 groundwater (commonly taken as a reference water composition in Yucca Mountain hydrochemical studies). Standard deviations of the pore water analyses are also shown. Pore water from the PTn is variable in composition, but the mean values of 11 representative analyses from boreholes UZ-16, UZ-14, and NRG-6 in mg/L are: Ca, 66; Mg, 13; Na, 42; Cl, 82; $HCO_3$, 82; $NO_3$, 25; and $SO_4$, 101. Comparison of these values with the mean and standard deviation values for the new pore-water analyses (Figure 18) shows that the major differences are in Cl, $SO_4$, $HCO_3$, and Na concentrations. The mean concentrations of dissolved ions in the pore waters are two to ten times the values for UE-25 J-13 water. (The 45° dashed line on Figure 18 is the loci of values that would be ten times those of the J-13 values.)

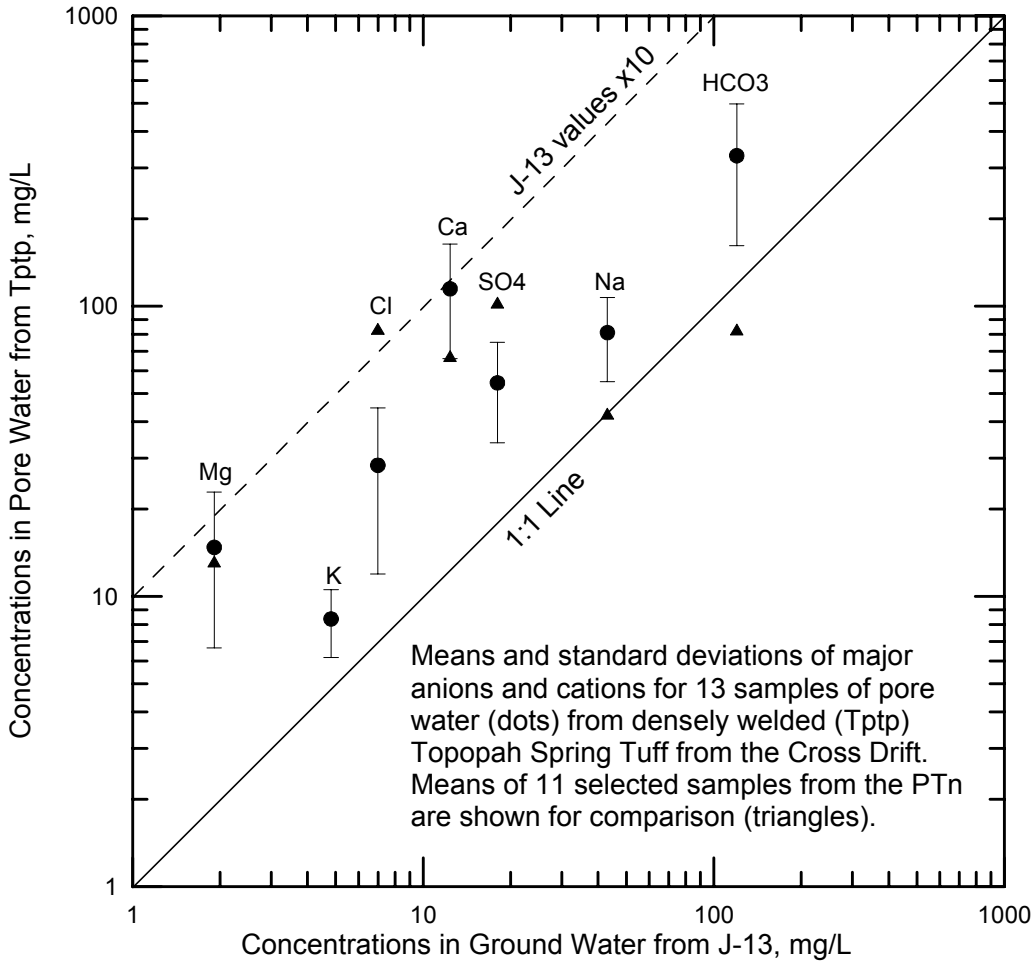


Figure 18. Comparison of Mean Pore-Water Composition Relative to Water from Well UE-25 J-13

### 3.6.4 Fluid Inclusions and Oxygen Isotopes

#### 3.6.4.1 Introduction

Fluid inclusion and O isotopic estimates of secondary mineral depositional temperatures coupled with geochronologic age determinations provide a record of past unsaturated zone temperatures. Additional work not captured in the current YMS&ER (DOE 2001a) is discussed below.

#### 3.6.4.2 Summary of Information Supporting the YMS&ER and YMPSSE

Secondary calcite within the Yucca Mountain unsaturated zone has been interpreted as a precipitate from films of water of meteoric origin percolating downward through the unsaturated zone fracture network (Paces et al. 2001). However, fluid inclusions hosted by secondary calcite in the unsaturated zone and indicating depositional temperatures in excess of modern ambient conditions were reported in 1996 and attributed to upwelling of hydrothermal fluids into the unsaturated zone (Dublyansky et al. 1996). These findings and interpretation spurred concurrent but independent comprehensive studies of the petrology and thermochronology of calcite-hosted fluid inclusions by the University of Nevada, Las Vegas and the U.S. Geological Survey. The results of these studies were presented to the Nuclear Waste Technical Review Board in April 2001 and at the International High-Level Radioactive Waste Management Conference in May 2001 confirming the origin of the secondary minerals from descending water under unsaturated conditions (Whelan et al. 2001) and verifying elevated depositional temperatures in the past (Whelan et al. 2001; Wilson and Cline 2001).

#### 3.6.4.3 Summary of Recent Test Results and Other Additional Information

Temperatures of unsaturated zone calcite formation estimated from two-phase fluid inclusions (crosses), from calcite $\delta^{18}O$ values (filled circles), and from U-He closure temperatures of apatite from an altered pumice clast are plotted against age. The depositional timing of some of this calcite has been determined from the radiometric ages of opal or chalcedony ($^{230}Th/U$ or U-Pb) and apatite (U-He) (Figure 19). The wide descending field is a best-fit curve to the $\delta^{18}O$-based temperatures, assuming depositional water $\delta^{18}O$ values of -13 to -11‰. The plot shows a long-term cooling trend, from temperatures near 80°C (176°F) at about 10 million years (Ma) to temperatures near modern ambient conditions beginning about 3 to 4 Ma and continuing into the present.

## 3.7 NATURAL ANALOGUES

### 3.7.1 Introduction

Studies of natural and anthropogenic analogues are used to test and build confidence in process models. In this sense, analogues have been used to corroborate the operative processes of the unsaturated zone flow and transport models as one line of evidence, among others, of the long-term operation of processes at scales too large to measure by laboratory and field-scale experiments. Analogues are also used to investigate the degree to which that modeling codes represent the processes correctly and that they provide reasonable matches to observed data.

Both qualitative and quantitative applications of natural analogues have been used by the Yucca Mountain Site Characterization Project. Examples of both types are given in this section.

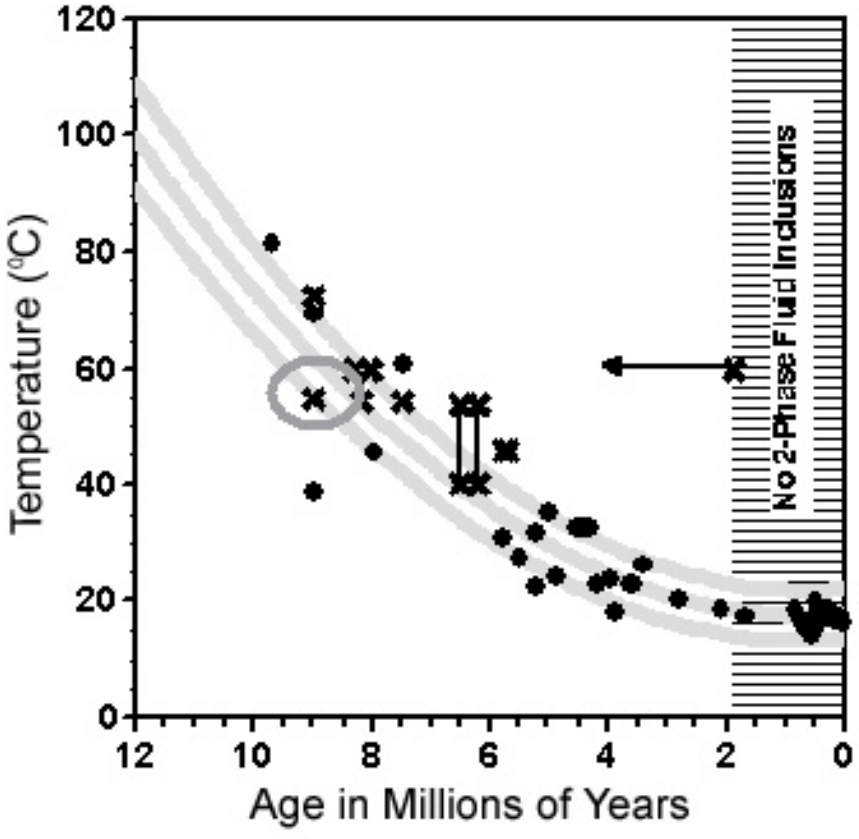


Figure 19. Temperatures of Calcite Deposition from Fluid Inclusion Homogenization Measurements (Crosses), $\delta^{18}O$ Values (Circles), and Apatite He-Diffusion (Large Oval) Plotted against Depositional Ages Determined from Associated Opal or Chalcedony ($^{230}Th/U$ or U-Pb) or Apatite (U-He). The arrow indicates a minimum timing for deposition of the fluid inclusions measured in that sample. The lines connect bimodal fluid inclusion temperature distributions within individual samples; in these samples the lower temperature inclusions are paragenetically younger than the higher temperature inclusions.

### 3.7.2 Summary of Information Supporting the YMS&ER and YMPSSE

Volume 1 of *FY01 Supplemental Science and Performance Analyses* (BSC 2001a) included multiple lines of evidence for all of the processes included in the unsaturated zone flow and transport models, including the effect of heat on drift-scale and mountain-scale coupled processes. This included information derived from the natural studies done at that time.

**Geothermal Analogues for Mountain-Scale**—Numerical modeling plays a crucial role in understanding the impact of heat on the performance of the unsaturated zone at the mountain scale. The justification of model approaches employed in the unsaturated zone model, and the validity of their results, depends on the successful modeling of fluid and heat transport in large geothermal systems, for which an extensive volume of field data are available to provide model

validation. Table 3.3.5.2 in *FY01 Supplemental Science and Performance Analyses* documented recent applications of TOUGH2 in modeling geothermal systems (BSC 2001a, pp. 3 to 12). These have increased confidence in the numerical approaches used in the unsaturated zone model.

### 3.7.3 Summary of Recent Test Results and Other Additional Information

**Seepage**—Examples of measured seepage in caves at Altamira, Spain, and Kartchner Caverns, Arizona, indicated, in each instance, that less than 2 percent of the available moisture became seepage (BSC 2001a, Section 4.3.1.7). Although quantitative measurements such as these are uncommon, examples provided abundant qualitative evidence that underground openings in the unsaturated zone divert much infiltration, thereby preserving fragile artifacts and remains as well as cave paintings. These analogues add supporting evidence that infiltration will be diverted around repository drifts at Yucca Mountain.

Additional examples have been found since the *FY01 Supplemental Science and Performance Analyses* (BSC 2001a), which indicate limited seepage in caves with moderate (Carlsbad, New Mexico) to very high precipitation rates (Ajanta, India). In addition to showing that most infiltration does not become seepage, natural analogues demonstrate that much of the seepage that does occur stays on the roof and walls of the opening rather than dripping into the opening. Examples of this are found at Goreme, Turkey, and at one of the buildings at the Denver Federal Center. Furthermore, if relative humidity is kept below 100 percent through ventilation, then seepage of liquid water is reduced or completely suppressed (BSC 2001a, pp. 4 to 6). Most caves are close to, but below, 100 percent relative humidity (e.g., Kartchner RH = 99.4 percent [Buecher 1999, p. 11]); thus, the amount of seepage would be expected to be low.

**Idaho National Engineering and Environmental Laboratory**—The Large-Scale Aquifer Pumping and Infiltration Test conducted at the Idaho National Engineering and Environmental Laboratory was modeled using TOUGH2 to simulate the highly transient water infiltration, ponded-water conditions, and conservative selenium ($^{75}$Se) tracer transport in the fractured basalt and sedimentary interbeds at the site. Six ponded-water hydrographs measured during the infiltration test were used during calibration with ITOUGH2 to estimate six parameters that controlled unsaturated flow in the fractured basalt and dense clay sedimentary interbed underlying the basalt flow. The estimated parameter values were within the range of data measured from cores obtained in the field, thus substantiating the physical relevance of the calibration effort. Successful calibration of the flow model helped to build confidence in the dual-permeability approach used to represent the fracture and matrix continua of the basalt in simulation of transient unsaturated flow (Figure 20). Two of these hydrographs, with associated $^{75}$Se breakthroughs, were then used in a joint flow–transport calibration.

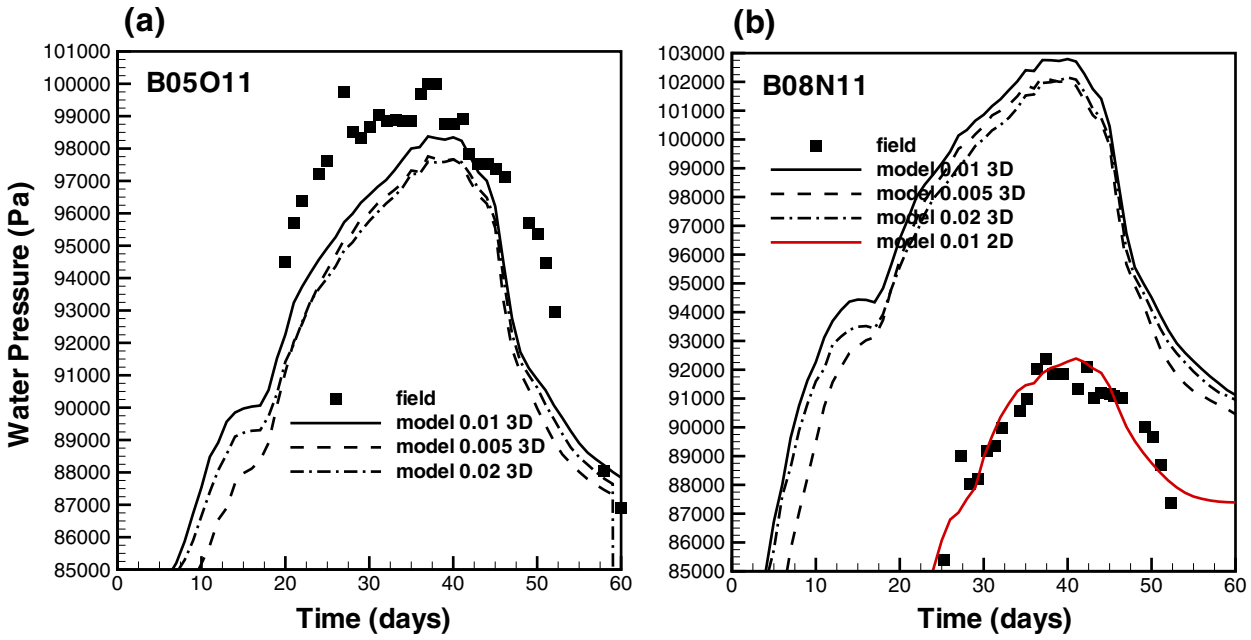


Figure 20. (a) Predictive Model Results for Control Hydrograph B05O11 and (b) Predictive and Calibration Results to Hydrograph B08N11. Symbols represent hydrograph data; lines represent model results. [Scientific Notebook SN-LBLN-SCI-186-V1 (YMP-LBNL-AMS-NA-AJ-2) p. 44]

**Geothermal Analogues for Mountain-Scale**—Literature review conducted since publication of *FY01 Supplemental Science and Performance Analyses* (BSC 2001a) focused on the relevance of geothermal analogues to thermal-hydrologic-chemical processes at Yucca Mountain. Dozens of geothermal fields were surveyed as to their ability to address such processes as advective heating, conductive heating, fracture-dominated fluid flow, chemical transport, boiling, dryout, condensation, mineral dissolution, and mineral alteration and precipitation. Differences between most geothermal analogues and the potential Yucca Mountain repository were acknowledged. This review indicated that only a small portion of the fracture volume needs to be sealed to effectively retard fluid flow in low permeability rocks (such as the welded ash flow tuffs at Yucca Mountain) in which fluid flow is controlled by fractures. Furthermore, fracturing and sealing occur episodically in geothermal systems. Sealing can occur over a time frame of days to years, depending on which processes trigger the precipitation of minerals. Rates and volumes of mineralization are controlled by mineral solubilities, reaction rate kinetics, and the flux and chemistry of circulating fluids.

## 3.8 BUSTED BUTTE

### 3.8.1 Introduction

Interim results of the unsaturated zone transport test at Busted Butte have been reported in *Unsaturated Zone and Saturated Zone Transport Properties (U0100)* (CRWMS M&O 2001); *Unsaturated Zone Flow and Transport Model Process Model Report* (CRWMS M&O 2000a); and *Yucca Mountain Preliminary Site Suitability Evaluation* (DOE 2001b). Detailed descriptions of the test are available in *Unsaturated Zone and Saturated Zone Transport Properties (U0100)* (CRWMS M&O 2001) and other project reports.

### 3.8.2 Summary of Information Supporting the YMS&ER and YMPSSE

The unsaturated zone transport test was designed to address uncertainties associated with the TSPA site-process models. The test involved field-scale tracer injection tests, laboratory analysis of pads collecting tracer from the field, and computational modeling to test the conceptual models being used for the Yucca Mountain Site Characterization Project. The unsaturated zone transport test was composed of two phases. Phase 1 included two 1-meter-scale in situ experiments to study specific processes, while Phase 2 was a 10-meter-scale experiment to assess the flow and transport response as a whole. Computational models of Phase 2 were run prior to the beginning of injection, as blind predictions, and during the course of injections, as more data became available against which to validate the model. Updating of the conceptual model and the geologic structure continue following termination of injection, as data continue to become available from continuing laboratory analyses, and mineback of the test block. Computational grids were generated based on pre-mineback physical data and were updated as additional information became available.

The unsaturated zone transport test has focused on addressing the original six test objectives:

1. Quantify the effect of heterogeneities on flow and transport in unsaturated and partially saturated conditions in the Calico Hills Formation (Tac)

2. Address issues relevant to fracture-matrix interactions and permeability contrast boundaries

3. Understand migration behavior of colloids in fractured and unfractured areas of the Calico Hills Formation

4. Validate transport modeling and predictions through field testing of laboratory sorption experiments in the unsaturated Calico Hills Formation

5. Evaluate the three-dimensional site-scale flow and transport process model used in the performance assessment abstractions for license application

6. Validate scaling assumptions made when moving from lab scale to field scale and site scale.

The YMPSSE (DOE 2001b) presented the results from the unsaturated zone transport test, available through February 2001, as they related to each of the unsaturated zone transport test goals. By that time, injection was completed, overcoring of injection holes was completed, and the Phase 2 mineback had just started. Pad analyses from the injection were continuing, and rock analyses had just commenced. A partial mineback of the Phase 2 test block provided an additional means to identify tracer movement and the role of structure on flow and transport. A large suite of simulations for Phase 2 was run and presented to understand dominant flow and transport processes in the test block, and to assess the ability of the model to capture site scale behavior.

### 3.8.3 Summary of Recent Test Results and Other Additional Information

This section provides a brief summary of results from the unsaturated zone transport test not included in other documentation to date. Results are presented against each of the objectives listed in the previous section.

To assess colloid transport in the unsaturated zone, polystyrene microspheres were injected as part of the tracer mixture as surrogate colloids. Microsphere migration has also been analyzed in laboratory cores and in overcore samples. In the laboratory, a mixture of microspheres and LiBr was used. Under saturated conditions in the laboratory, the percent mass recovered for 190 nm microspheres within the Tac samples varied as a function of ionic strength, with 21 percent recovered at 0.01 M LiBr and 36 percent at 0 M. In contrast, 44 nm microspheres had up to 82 percent recovery in the same material, indicating that the smaller colloids can migrate easier through this material. Qualitative assessment of in situ microsphere transport in the overcores taken around and below injection boreholes showed transport of approximately 0.21 m (0.69 ft) below the 50 ml/hr injectors over the 800-day injection period. From these rock analyses, it is not possible to distinguish between the two sizes of microspheres injected.

A new model developed for colloid transport under the unsaturated zone transport test allows four different physical mechanisms for colloid transport. Based on very-high-resolution characterization of Tac pore space, this model predicts a travel distance of less than 50 m (164 ft) after 450 years for a 50 percent saturated system. The simulated conditions represent the physical Tac system as accurately as possible. Saturation is slightly higher (50 percent instead of estimated 35 percent in situ pre-unsaturated zone transport test), which would increase potential transport predictions over a lower saturation.

The Phase 1 field tests allowed a small-scale analysis of the effects of permeability contrast boundaries (faults/fractures, layer interfaces). Flow was matrix dominated. The field tracer results showed that layers and interfaces appeared to delay movement of the tracer, and there has been no evidence of fractures/faults enhancing transport in the CHn units.

Pad analysis from Phase 2 has demonstrated that heterogeneity affects spatial distribution of moisture and tracers at high resolution (centimeters to meters). At the field scale, Phase 2 data show linear travel distance with time over distances of 0.3 to 3 m (0.9 to 9.8 ft).

Analyses to date indicate that laboratory hydraulic conductivities likely underrepresent Tac and Tptpv1 field conductivities by 2 orders of magnitude, and possibly more.

The results of the transport of metal tracers injected during Phase 2 are just becoming available from overcore rock sample analyses. The metals Ni, Co, and Mn were used as surrogate radionuclides, representing Am, Pu, Tc, and Np. Samples below the highest injection rate holes (50 ml/hr) have been analyzed. This injection rate is far higher than any expected ambient flow. Cobalt has traveled approximately 0.3 m (0.9 ft) below the injector, while Ni concentrations elevated above background have been observed approximately 0.15 m (0.49 ft) below the injector.

Prior to incorporating stratigraphic detail from the mineback, the simulation results matched the general character of the tracer distribution well. Representation was better for near-field

collection boreholes and for boreholes in the Tac. In the Tac, injection and collection boreholes generally reside within the same unit. More accurate geologic representation in the computational grids has produced improved prediction.

The AECL laboratory transport testing is using the following tracers/isotopes: Na-fluorescein, $^{3}H$, $^{22}Na$, $^{60}Co$, $^{99}Tc$, $^{137}Cs$, and $^{237}Np$. The results of the AECL laboratory tests on the smaller (30-cm [12-in.]) block, obtained from elution profiles, showed that, relative to an ideal conservative tracer, $^{3}H_2O$, transport of technetium (injected as an anionic $TcO_4^-$ species) was approximately 15 percent faster, but that neptunium (injected as the neptunyl ion $NpO_2^+$) was retarded by a factor of approximately 3. Triay et al. (1996), Appendix A) conducted column experiments with crushed tuff and found neptunium breakthrough curves indicating retardation coefficients always greater than 1 and ranging up to approximately 4, depending on rock type. The AECL findings fall within this range. Retardation of $^{22}Na$, $^{60}Co$, and $^{137}Cs$ by the geological material was higher than for neptunium. Post-experiment radiometric analysis of the tuff, which is currently underway, shows that the order of retardation is $^{22}Na < ^{137}Cs < ^{60}Co$. This agrees qualitatively with the experimentally determined static batch sorption coefficients for these radioisotopes. Tracer breakthrough has not yet occurred in the larger (1 $m^3$) block test.

## 3.9 AN EXPECTED CASE MODEL OF UNSATURATED ZONE FLOW AND TRANSPORT

### 3.9.1 Introduction

The unsaturated zone flow and transport model is the culmination of much data collection and analysis, conceptual model development, and numerical model calibration and covers the entire unsaturated zone from the well-characterized near-surface rocks to the poorly-characterized rocks near the water table. As a result, there is substantial uncertainty about portions of the model, particularly in the Calico Hills nonwelded hydrogeologic unit (CHn) and the Crater Flat undifferentiated hydrogeologic unit (CFu), which are nearest the water table. In addition, due to the complexity of the physical system and processes, simplifications are necessary for modeling flow and transport. Following standard engineering practice, these uncertainties and simplifications have been treated conservatively so that confidence in the model results is as high as possible.

As part of an overall emphasis on the best characterization possible of uncertainties, an Expected Case model was developed. As documented in *Unsaturated Zone Flow Patterns and Analysis* (BSC 2001b), a series of studies were conducted to evaluate the impact of conservatism used as a result of uncertainty and simplification. Scenarios judged to be most likely, or expected, are compared to the previously used conservative scenarios.

### 3.9.2 Summary of Information Supporting the YMS&ER and YMPSSE

The unsaturated zone flow and transport model uses a dual-permeability model approach in which global flow may occur in either the fracture or the matrix continuum. Flow between the two continua is also allowed. Where a steady-state flow assumption is valid, a dual-permeability model approach can accurately reproduce conditions in the unsaturated zone. Transport modeling using the dual-permeability model approach, however, may result in breakthrough

times that are underestimated, because the diffusive gradient from the fracture to the matrix continuum, and thus the retardation potential of the matrix, is underestimated.

Several transport codes have been used to simulate natural tracers and releases of radionuclides from the potential repository. TSPA analyses have been conducted using the particle tracking code FEHM, which uses a residence time/transfer function approach where particles are only carried by advection and the effects of matrix diffusion on fracture flow are accounted for by a modified residence time in the fractures. Particles that diffuse into the matrix can not then be transported by matrix advection. Much of the unsaturated zone flow and transport model comparison and calibration to natural tracers and also predictions of travel times from the repository horizon to the water table are carried out using T2R3D, which when used with a dual-permeability model approach and the relatively coarse discretization of the unsaturated zone flow and transport model, underestimates diffusive flux from the fracture to the matrix continuum and suffers from numerical dispersion. Both of these effects contribute to breakthrough times that are underestimated. DCPT V1.0 is another code used for transport calculations, which, like FEHM, uses the particle tracking approach to overcome the numerical dispersion inherent in the coarse discretization of the unsaturated zone flow and transport model. While DCPT V1.0 suffers from underestimation of the diffusive gradient into the matrix, it does allow particles, which diffuse into the matrix to then be advected in the matrix continuum.

Characterization of the fracture continuum relies on observation of the number of fractures on the surface and underground in tunnels and boreholes, air-injection and gas tracer testing in boreholes, and passive observation of barometric pumping effects. These types of data are readily available for the TCw, PTn, and TSw. However, for the CHn and CFu, the data are sparse. Furthermore, the assumption that the fractures are essentially dry, which vastly simplifies the analysis of the air-injection testing and barometric pumping data, is invalid for the areas in the CHn and CFu where perched water is present. Because of the sparseness of data, fractures in the CHn and CFu are mainly characterized as being analogous to fractures in similar units in the better-characterized portions of the mountain. The fractures in the CHn and CFu are considered to be globally connected in a continuum and generally more permeable than the matrix allowing continuous fracture continuum flow from the repository horizon to the water table. As a result, transport simulations show a very early time breakthrough of radionuclides at the water table. Additionally, for simulation of transport, radionuclides are released directly into undisturbed fracture flow at the repository horizon.

### 3.9.3 Summary of Recent Test Results and Other Additional Information

As an alternative to the dual-permeability approach, Pruess and Narasimhan (1985) proposed the multiple interacting continua (MINC) approach. In this approach, the matrix is discretized into multiple grid blocks allowing resolution of gradients between the fractures and the matrix and more accurate simulation of transient flow and diffusion. Figure 21 shows a schematic of a proposed application of the MINC approach for simulation of unsaturated zone flow and transport at Yucca Mountain. Because of the increased number of grid blocks, six MINC grid blocks for every two dual-permeability model grid blocks, computational efficiency is much reduced.

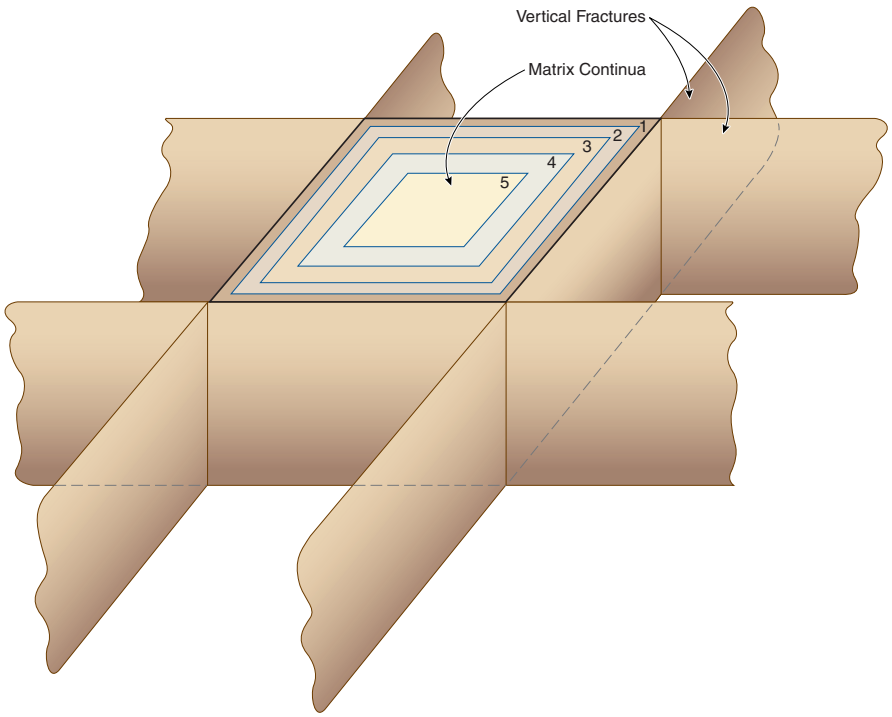


Figure 21. Matrix Discretization for the MINC Scheme Used in this Study

The MINC approach is compared to the dual-permeability model approach, using a two-dimensional, east-west cross section that intersects borehole USW UZ-14. This cross section is selected because the CHn is entirely zeolitized, and, thus, matrix diffusion will be emphasized in transport simulations. Flow simulations and comparison of resulting saturation and water potential show that for steady-state flow the dual-permeability model and MINC approaches are nearly identical. Where matrix properties of adjacent layers are very different (e.g., at the interface between the PTn and TSw) differences were noted in the flow simulations but were localized to the interface areas. Simulations of transport from the repository horizon to the water table of a conservative tracer with a molecular diffusion coefficient of $3.2 \times 10^{-11}$ $m^2/s$ show vastly different results. Figure 22 shows a 20 percent breakthrough time of approximately 20 years using the base-case dual-permeability model approach for the selected cross-section, while with the MINC approach a 20 percent breakthrough time of approximately 10,000 years is achieved. Note that these simulations do not include the effects of the vitric CHn, perched water, or faults.

The particle-tracking code DCPT has been modified to incorporate an approximation of the non-linear matrix diffusion gradient as presented by Pan and Bodvarsson (2001). With this modification DCPT V2.0 has both the advantages of particle trackers (i.e., no numerical dispersion and computational efficiency) and better representation of matrix diffusion that is fully coupled with matrix advection. A comparison between DCPT V1.0 and DCPT V2.0 for transport of both conservative (Tc) and nonconservative (Np) species from the repository horizon and the water table using the unsaturated zone flow and transport model, shown in Figure 23, demonstrates the benefit of better representation of matrix diffusion. Note that this comparison does include some of the effects of the vitric CHn and faults.

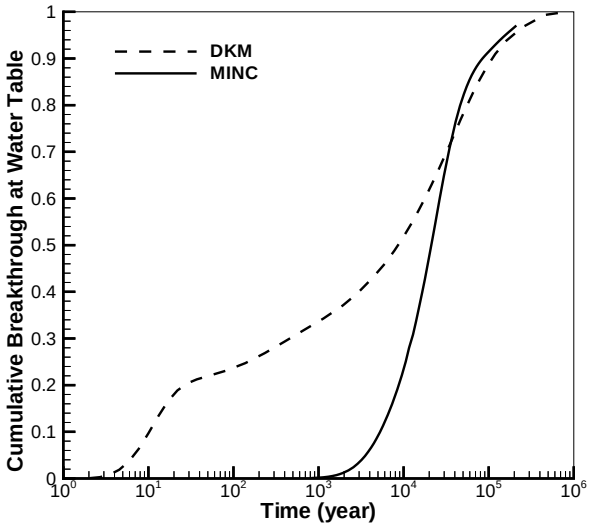


Figure 22. Prediction of Cumulative Breakthrough of a Conservative Tracer at the Water Table Using a Two-Dimensional Model and the Dual-Permeability Model and MINC Approaches

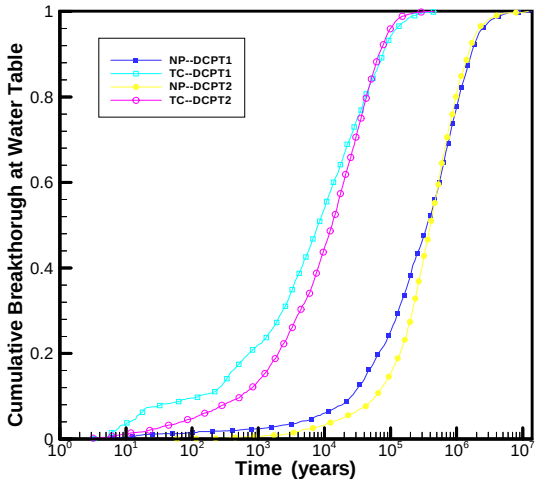


Figure 23. Comparison of Predictions Using the Unsaturated Zone Flow and Transport Model and DCPT V1.0 (DCPT1) or DCPT V2.0 (DCPT2) of Cumulative Breakthrough of Conservative (Tc) and Nonconservative (Np) Tracers at the Water Table

The model of a continuous, well-connected fracture network was reevaluated for the CHn. Data from Busted Butte, presented above in Section 3.8, indicate that flow in the vitric portion of the CHn (CHn(v)) is entirely in the matrix, likely because of high matrix permeability and capillarity in the matrix that is greater than that in the fractures. Additionally, based on reevaluation of the conceptual model of the fracture network in the CHn, a more likely model is that the well-connected fracture network in the CHn is relatively sparse. Application to the unsaturated zone flow and transport model resulted in two changes: (1) fractures were removed from the CHn(v) in order to force all flow into the matrix, and (2) fracture permeability in the zeolitic, northern areas associated with perched water were increased an order of magnitude (resulting in

a two order of magnitude difference between fracture and matrix permeability). These two changes result in a more consistent model of a sparsely-connected fracture network in the CHn; in the zeolitic northern areas associated with perched water the large contrast between matrix and fracture permeability forces flow into the fractures, which are just impermeable enough to support the observed perched water, while in the CHn(v) flow is entirely in the matrix because it is at least as permeable as the fractures and has a greater capillarity.

The effect of two further modifications which approximate more likely scenarios are also evaluated. First, a conservative matrix diffusion coefficient corresponding to that of technetium (Tc) has been used in previous simulations. A higher coefficient corresponding to that of tritiated water may be more representative of the range of radionuclides expected to be released from the potential repository. Second, because the emplacement drifts may act as capillary barriers, the rock immediately below the drifts may have reduced saturation and flow especially in the fractures. This effect is demonstrated for uniform percolation in a homogeneous, isotropic, porous media by Philip et al. (1989). Radionuclides released in the drift are more likely to be transported away from the drift by diffusion or advection in the matrix until areas of greater fracture flow are encountered. A very simple analysis of the potential effect is carried out by releasing radionuclides to the matrix rather than the fractures at the repository horizon.

A comparison of the cumulative effects of these modifications is shown in Figure 24. Removing the fractures from the CHn(v) results in an increase of the 20 percent breakthrough time from approximately 300 to 500 years (curves (a) and (b)). Adding an increase to the fracture permeability in the zeolitic areas and an increase to the molecular-diffusion coefficient increases the 20 percent breakthrough time to approximately 2,000 years (curve (c)). Curve (c) is the current best estimate of for breakthrough times between the potential repository and the water table. Finally, adding the release of the radionuclides to the matrix increases the 20 percent breakthrough time to approximately 6,000 years (curve (d)).

## 3.10 USE OF DISCRETE FRACTURE NETWORK MODEL FOR MODELING FLOW FOCUSING AND SEEPAGE

### 3.10.1 Introduction

Flow focusing and seepage into drifts are important factors affecting the performance of the potential repository in the unsaturated zone of Yucca Mountain. This section summarizes simulation results for flow focusing and seepage processes based on a discrete fracture network model.

### 3.10.2 Summary of Information Supporting the YMS&ER and YMPSSE

Issues related to flow focusing and seepage are presented in detail in Section 3.3.2.4 of YMPSSE (DOE 2001b) and Section 4.2.1.3 of YMS&ER (DOE 2001a). A summary of the key model processes for seepage is also given in Section 3.4.2 of this report. However, in the relevant modeling studies reported in YMS&ER and YMPSSE, continuum approaches were used. The use of discrete fracture network model provides further insights of flow focusing and seepage processes in unsaturated zone and is useful for evaluating uncertainties involved in the previous modeling results.

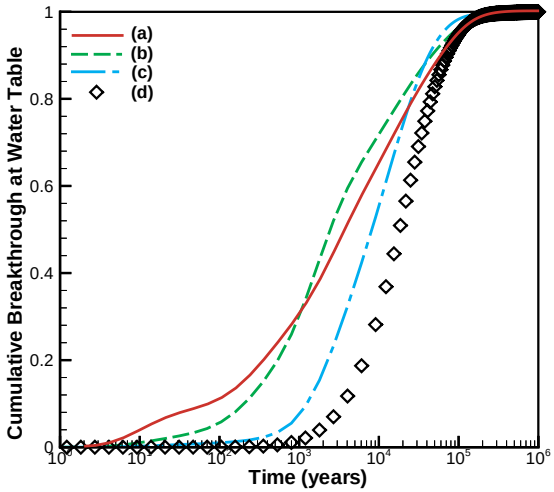


Figure 24. Comparison of Transport from the Repository Horizon to the Water Table for Several Modifications to the Unsaturated Zone Flow and Transport Model: (a) base-case model with continuous, well-connected fractures through the CHn(v), the permeability-barrier model for perched water, a molecular-diffusion coefficient of $3.2 \times 10^{-11}$ $m^2/s$, and release of radionuclides to the fractures; (b) base-case model modified by removing fractures from the CHn(v); (c) model (b) modified by increasing the fracture permeability for perched water by a factor of 10 and increasing the molecular-diffusion coefficient by a factor of five; (d) model (c) modified by releasing the radionuclides to the matrix.

### 3.10.3 Summary of Recent Preliminary Modeling Results and Other Additional Information

Figure 25 shows a computationally generated two-dimensional fracture network consisting of sub-vertical and sub-horizontal fractures. The orientations and trace lengths are consistent with fracture map data collected from detailed line surveys for Topopah Spring welded (TSw) unit. Fractures with trace lengths smaller than 0.23 m were not considered in this study. Hydraulic properties of individual fractures are related to their trace lengths. Longer fractures are considered to have larger apertures and therefore smaller air entry values. Intersections between fractures and the outline of a drift are also shown in Figure 26. The entire (or partial) top boundary of the network is connected to a single source assigned a flow rate corresponding to a percolation flux of 5 mm/yr (0.2 in./yr).

Figure 26 shows steady-state flow paths when all fractures intersected with top boundary are connected to the percolation source element. In Figure 27, only a portion of fractures at the top boundary is connected to the source element to demonstrate effects of flow focusing that develop above the top boundary.

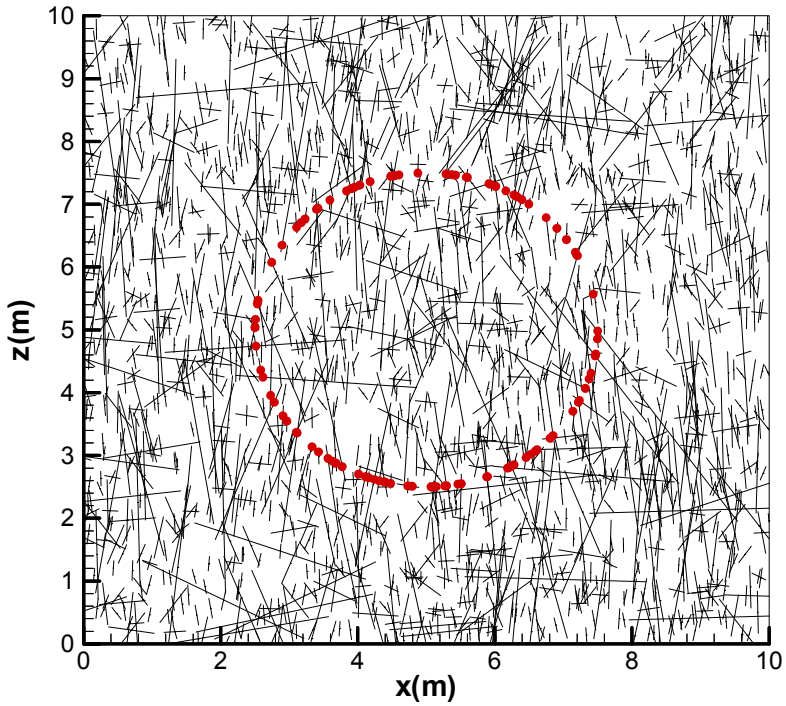


Figure 25. A Computationally Generated Fracture Network. The solid circles correspond to intersections between fractures and the outline of a drift.

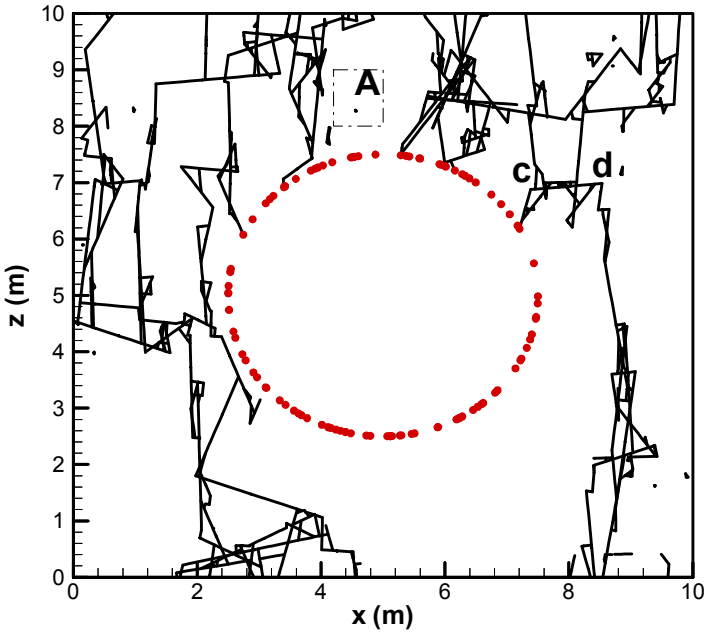


Figure 26. Steady-State Flow Paths in the Unsaturated Fracture Network. The solid circles correspond to intersections between fractures and the outline of a drift. Zone A contains a group of small fractures that do not take part in the global flow.

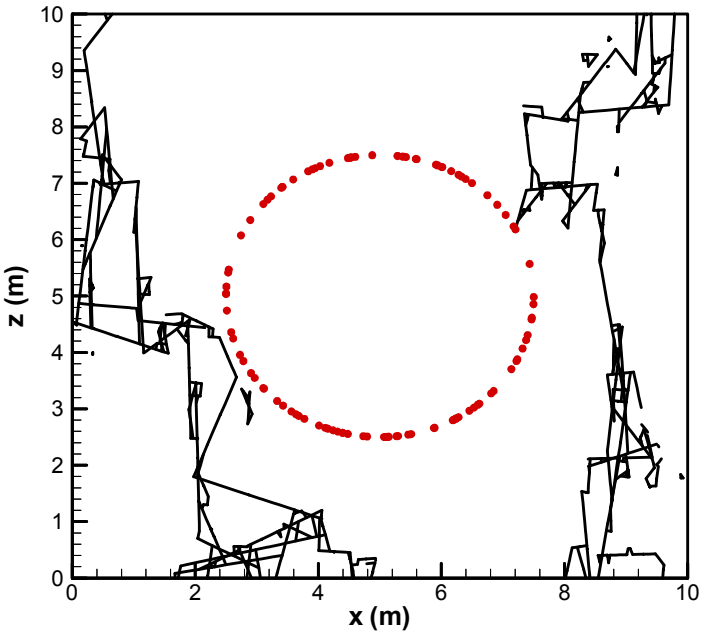


Figure 27. Steady-State Flow Paths in the Unsaturated Fracture Network when only a Portion of Fractures at the Top Boundary (Located Between 0 to 1.5 m and Between 8.5 to 10 m in the Horizontal Direction)

# 4. IMPLICATIONS OF RECENT TEST RESULTS AND OTHER ADDITIONAL INFORMATION

## 4.1 SYSTEMATIC HYDROLOGIC CHARACTERIZATION

The results in the lower lithophysal unit confirm the understanding of unsaturated zone flow in the repository units as described in YMS&ER (DOE 2001a) and YMPSSE (DOE 2001b), based previously on niche test results in the middle nonlithophysal unit. The systematic hydrologic characterization focuses currently in the lower lithophysal zone of TSw for seepage quantification with long boreholes along the Cross-Drift under different ventilation conditions. The recent test results indicate that the seepage threshold is considerably higher in the lower lithophysal unit than in the middle nonlithophysal unit. Therefore, seepage in potential waste emplacement drifts in the lower lithophysal unit is expected to be lower than in the middle nonlithophysal unit. The small fractures connected by lithophysal cavities constitute the main contribution to liquid flow, and the water drainage is expected to be good.

## 4.2 CROSS-DRIFT BULKHEAD MOISTURE MONITORING AND SEEPAGE OBSERVATIONS

The water observed behind the bulkheads is believed to result from condensation (originating as pore water and/or construction water) related to temperature variations in the drifts. The available chemical analyses support this hypothesis.

## 4.3 PRELIMINARY OBSERVATIONS FROM THE FAULT TEST AT ALCOVE 8/ NICHE 3

This new testing program has provided preliminary observations of how water flows through a fault located within fractured, welded units within Yucca Mountain. Our current observations have included travel velocities within the fault and some indications of the magnitude of wetted-plume dispersion following localized releases in the fault. The wetting front travel time over a distance of 20 m (66 ft) is of the same order of magnitude as the travel time over 30 m (100 ft) observed at Alcove 1. The plume is fairly localized as indicated by measurements in the borehole sensor and from observations of seepage exit points on the Niche 3 ceiling.

## 4.4. SEEPAGE TESTING AT NICHES

Evaporation losses during the liquid-release tests have been identified as a potential systematic error in the measured seepage rates, and thus in the parameters derived from these data. The evaporation loss measurements collected both in Niche 4 and in Cross-Drift Niche 5 are used to quantify the effects of this process and thus allow for correction of seepage test results.

The results of recent analyses of long-term seepage threshold tests under controlled relative humidity conditions are consistent with the results of early analyses of short-term tests on open niche. The seepage threshold concept is demonstrated in both conditions. The preliminary seepage test at Cross-Drift Niche 5 suggests that the lower lithophysal zone of TSw has large capacity to suppress seepage. Whether this result is due to strong storage effect or due to seepage diversion remains to be resolved (by water collection in the newly excavated slot on the niche wall or by other testing approach.)

## 4.5 CHLORINE-36 AND TRITIUM

Comparison of the chlorine-36 and tritium data within the ESF yields several apparent discrepancies. While the chlorine-36 data indicate the presence of post-bomb chlorine-36 at numerous locations within the Drill Hole Wash and Sundance faults, the tritium data indicate that only one of 52 samples from those faults contained detectable traces of post-bomb tritium. In addition, the chlorine-36 data indicate that the south ramp is devoid of any post-bomb water, where as the tritium data indicate that post-bomb water is common within the south ramp.

The discrepancy noted in the Sundance and Drill Hole Wash fault areas may be the result of evaporation. When the water evaporates, it does not leave a precipitate behind because tritium is part of the water molecule. Chlorine is transported as a solute and remains behind as a mineral precipitate when the water evaporates. This precipitate is then available for analysis after the rock is leached. If evaporation is the responsible mechanism, the implication is that the volume of water entering the system through these fast pathways is extremely small and is almost entirely removed by evaporation.

In the south ramp, the differences between the chlorine-36 and tritium laboratory are more difficult to explain. The most likely explanation would appear to be excessive leaching of the samples prior to chlorine-36 analysis. This would dilute any post-bomb isotopic signature by the addition of very old rock chloride. Another possible explanation is a masking of the bomb-pulse

signal in areas with matrix pore waters that have high chloride content (Sonnenthal and Bodvarsson 1999).

## 4.6 UNSATURATED ZONE CHEMISTRY

### 4.6.1 Calcite Abundances

The differences in calcite abundances between the two boreholes indicate that the TSw experienced different amounts of unsaturated zone flow at the two different sites. Spatial variations in unsaturated zone flow may be the result of several different factors including differences in infiltration rates or other hydrogeologic factors affecting vertical flow. Infiltration at WT-24 may be slightly greater than at SD-6 due to a slightly higher elevation and a somewhat larger local catchment. However, both sites are modeled with similar infiltration and percolation values (DOE 2001a, Figures 4-25 and 4-27). Therefore, other hydrogeologic factors may be important for explaining the differences in calcite-abundance profiles. The higher calcite abundances in deeper units in WT-24 may be related to localized infiltration along nearby Yucca Wash, which is at an elevation equivalent to the lower parts of the Tptr in the borehole (near the depth below which calcite abundances increase dramatically). The lower apparent percolation fluxes in deeper TSw units at SD-6 also may reflect dispersal and slowing of vertical fracture flow in the Tptpul, where downward percolating water may be partially removed by an upward migrating gas phase (Paces et al. 1998). Because SD-6 is closer to central Yucca Mountain, the SD-6 calcite-abundance profile may be more representative of unsaturated zone flow within the potential repository block than the profile at WT-24. If this is the case, the calcite-abundance data may support lower flux rates than those given in the YMS&ER (DOE 2001a). Therefore, other hydrogeologic factors may be important.

### 4.6.2 Estimates of Seepage from Calcite

Observations of calcite deposits have been used to estimate seepage rates into lithophysal cavities. This approach provides an independent evaluation of seepage into open cavities averaged over the approximately 10-million-year history of Yucca Mountain. Due to differences in geometry between lithophysal cavities and potential waste emplacement drifts, as well as uncertainties in the estimation method, the seepage estimate based on calcite observations represents a lower bound for the seepage rate expected for potential waste emplacement drifts. The seepage rate determined from calcite observations is substantially lower than predicted by the TSPA model at the same seepage fraction. Therefore, the independent estimate for seepage from calcite data is consistent with TSPA seepage predictions given that (1) the TSPA model is a conservative predictor of seepage (i.e., favors higher seepage where uncertainty is not specifically quantified) and (2) the calcite approach can only provide a lower bound for seepage into potential waste emplacement drifts.

### 4.6.3 Pore-Water Geochemistry

Where multiple samples of water have been obtained from a single core hole, the analyses indicate significant compositional variation at the meter scale or finer. These spatial compositional disparities are not being erased by molecular or mechanical dispersion. Chloride concentrations in the new analyses (14 to 51 mg/L) are consistent with those reported in the

YMS&ER (DOE 2001a). In contrast with perched and saturated zone groundwater, most of the pore-water samples have Ca concentrations in excess of Na concentrations. The general agreement in chlorine contents of the new analyses with values used in the model at the potential repository level suggest that the impact of the additional data will be one of refinement rather than gross change.

### 4.6.4 Fluid Inclusions and Oxygen Isotopes

These results confirm a prolonged cooling of the unsaturated zone rock mass as predicted by modeling of unsaturated zone temperatures, based on the inferred position and thermal inputs from the magma chamber under the Timber Mountain caldera just north of Yucca Mountain (Marshall and Whelan 2000; Marshall and Whelan, in press). They also corroborate the fluid inclusion evidence that the unsaturated zone rock mass has been at or near modern ambient temperatures for the last several millions of years and that the thermal inputs responsible for the elevated temperatures in the past are no longer present.

The precipitation of secondary calcite and silica from fluids moving through the unsaturated zone during cooling of the tuffs is an analogue to conditions attendant with far-field heating of tuffs in a repository. Higher thermal gradients associated with a repository would result in a mobilization of fluids, possible causing local dissolution and reprecipitation of calcite and silica. Nonetheless, the results of the thermal history analysis from fluid inclusion studies, coupled with the sparse distribution of the calcite and silica formed during the past 10 million years or more, suggest that redistribution of minerals at these temperatures (up to 80°C [176°F]) would be unlikely to affect the hydrology of the repository block.

## 4.7 NATURAL ANALOGUES

The additional information reported here confirms and strengthens aspects of the unsaturated zone flow and transport models reported in *FY01 Supplemental Science and Performance Analyses* (BSC 2001a). Additional observations and data from caves and underground openings continue to suggest that seepage rates will be low or negligible if the relative humidity of the repository is kept below 100 percent. The Idaho National Engineering and Environmental Laboratory study provided added confidence in dual-permeability approaches to modeling flow in variably saturated media and confirmed the ability of the TOUGH2 family of codes to replicate field data of the Large-Scale Aquifer Pumping and Infiltration Test. The literature survey of geothermal fields with aspects similar to mountain-scale coupled processes at Yucca Mountain pointed out factors that determine the degree of thermal-hydrologic-chemical alteration. Results of the geothermal analogue survey suggest that fracture sealing should be expected at the drift scale in localized areas under hotter thermal loading scenarios. This would have implications for slowed fluid flow in the unsaturated zone model during the thermal pulse. The effect would be slight at the mountain scale and negligible at any scale in cooler repository designs. This survey noted again the lowered rate and degree of expected change in an unsaturated repository compared to a saturated geothermal field.

## 4.8 BUSTED BUTTE

1. Evidence indicates that flow and transport in the nonwelded to moderately welded tuffs evaluated in the unsaturated zone transport test (Tac, Tptpv1, Tptpv2) are matrix dominated. Fractures appear to play little, if any, role in enhancing flow and transport. However, faults and fractures may play a significant role as barriers to fluid and contaminant movement.

2. Comparison of tracer-transport data against model simulations indicates that laboratory-scale hydrogeologic parameters (saturated hydraulic conductivity, porosity, relative permeability, etc.) may deviate significantly from field-scale behavior. Modeling currently suggests a difference of possibly 2 or more orders of magnitude for hydraulic conductivity. These results suggest that the distribution of hydraulic parameters in the field have not been fully captured by laboratory-scale investigations. An increase in hydraulic conductivity of 2 orders of magnitude would produce more rapid transport in affected units.

3. Hydrogeologic parameters as measured in the laboratory are strongly biased by recoverability. Laboratory-scale hydrogeologic information about the Tac is still very limited because intact samples are virtually unrecoverable by common sampling techniques. This is a potentially a root cause of the errors discussed in Item 2, above.

4. Colloid transport in unsaturated conditions is much more limited than in saturated conditions. Long travel distances for any significant volume of colloids through the unsaturated zone is unlikely for colloids larger then 200 nm, but there is not enough information to evaluate the transport of smaller colloids.

5. Results to date of the rock-extraction studies show that reactive metals (Ni, Co, and Mn) are restricted to the environment adjacent to the injectors (cm scale), while Li and Br have migrated to the pad collection boreholes (meter scale). This suggests that the vitric Calico Hills provides significant retardation.

6. AECL results confirm that the transport behavior of the tracers and isotopes studied are consistent with expectations based on independent laboratory sorption and diffusion measurements.

## 4.9 AN EXPECTED CASE MODEL OF UNSATURATED ZONE FLOW AND TRANSPORT

The studies presented in *Unsaturated Zone Flow Patterns and Analysis* (BSC 2001b) serve two purposes. They confirm the conservatism of the models used for TSPA for Site Recommendation, and they demonstrate ways in which that conservatism can be reduced. Evaluation of a conceptual model of sparsely-connected fractures in the CHn shows increased breakthrough times at the water table. This model is considered more likely than the conservative model of well-connected fractures in the CHn. Finally, two model changes, increasing the molecular-diffusion coefficient and releasing radionuclides to the matrix (shadow zone effect), again result in increased breakthrough times. The higher rate of diffusion is more

realistic for representing tritium transport. The drift shadow effects on radionuclide transport are also considered more realistic.

## 4.10 USE OF DISCRETE FRACTURE NETWORK MODEL FOR MODELING FLOW FOCUSING AND SEEPAGE

**Flow Focusing**—Relatively sparse and mainly vertical flow paths dominate unsaturated flow in fracture networks. The top boundary condition (upstream flow focusing) has an extremely important effect on flow paths near drifts (see Figures 26 and 27), which has not been considered in previous modeling studies. Simulation results also indicate that focused flow paths persist through the network. An increase in flow focusing is expected to improve performance considerably because this will result in a reduction in the fraction of drifts that seep.

**Role of Small Fractures**—As indicated in Figure 26 (see Zone A), considerable portion of small fractures do not contribute to the global flow in unsaturated fracture networks. However, these small fractures are well connected with the global flow paths within a fracture network and with the tuff matrix, which may enhance the matrix diffusion.

## 5. REFERENCES


AP-2.14Q, REV 2, ICN 0. *Review of Technical Products and Data.* Washington, D.C.: U.S. Department of Energy, Office of Civilian Radioactive Waste Management. ACC: MOL.20010801.0316.

AP-SIII.1Q, Rev. 0, ICN 1. *Scientific Notebooks.* Washington, D.C.: U.S. Department of Energy, Office of Civilian Radioactive Waste Management. ACC: MOL.20000516.0002.

Ahlers, C.F.; Shan, C.; Haukwa, C.; Cohen, A.B.J.; and Bodvarsson, G.S. 1996. *Calibration and Prediction of Pneumatic Response at Yucca Mountain, Nevada Using the Unsaturated Zone Flow Model.* Milestone OB12M. Berkeley, California: Lawrence Berkeley National Laboratory. ACC: MOL.19970206.0285.

Bodvarsson, G.S.; Bandurraga, T.M.; and Wu, Y.S., eds. 1997. *The Site-Scale Unsaturated Zone Model of Yucca Mountain, Nevada, for the Viability Assessment.* LBNL-40376. Berkeley, California: Lawrence Berkeley National Laboratory. ACC: MOL.19971014.0232.

BSC (Bechtel SAIC Company) 2001a. *FY01 Supplemental Science and Performance Analyses, Volume 1: Scientific Bases and Analyses.* TDR-MGR-MD-000007 REV 00 ICN 01. Las Vegas, Nevada: Bechtel SAIC Company. ACC: MOL.20010801.0404; MOL.20010712.0062; MOL.20010815.0001.

BSC 2001b. *Unsaturated Zone Flow Patterns and Analysis.* MDL-NBS-HS-000012 REV 00. Las Vegas, Nevada: Bechtel SAIC Company. ACC: MOL.20011029.0315.

Buecher, R.H. 1999. "Microclimate Study of Kartchner Caverns, Arizona." *Journal of Cave and Karst Studies, 61,* (2), 108-120. Huntsville, Alabama: National Speleological Society. TIC: 249657.

CRWMS M&O (Civilian Radioactive Waste Management System Management and Operating Contractor) 2000a. *Unsaturated Zone Flow and Transport Model Process Model Report.* TDR-NBS-HS-000002 REV 00 ICN 02. Las Vegas, Nevada: CRWMS M&O. ACC: MOL.20000831.0280.

CRWMS M&O 2000b. *UZ Colloid Transport Model.* ANL-NBS-HS-000028 REV 00. Las Vegas, Nevada: CRWMS M&O. ACC: MOL.20000822.0005.

CRWMS M&O 2000c. *Calibrated Properties Model.* MDL-NBS-HS-000003 REV 00. Las Vegas, Nevada: CRWMS M&O. ACC: MOL.19990721.0520.

CRWMS M&O 2001. *Unsaturated Zone and Saturated Zone Transport Properties (U0100).* ANL-NBS-HS-000019 REV 00 ICN 1. Las Vegas, Nevada: CRWMS M&O. ACC: MOL.20010201.0026.

DOE (U.S. Department of Energy) 2001a. *Yucca Mountain Science and Engineering Report.* DOE/RW-0539. Washington, D.C.: U.S. Department of Energy, Office of Civilian Radioactive Waste Management. ACC: MOL.20010524.0272.

DOE 2001b. *Yucca Mountain Preliminary Site Suitability Evaluation.* DOE/RW-0540. Washington, D.C.: U.S. Department of Energy, Office of Civilian Radioactive Waste Management. ACC: MOL.20011101.0082.

Dublyansky, Y.; Reutsky, V.; and Shugurova, N. 1996. "Fluid Inclusions in Calcite from the Yucca Mountain Exploratory Tunnel." *Sixth Biennial Pan American Conference on Research in Fluid Inclusions, May 30–June 1, 1996.* Brown, P.E. and Hagemann, S.G., eds. Madison, Wisconsin: Department of Geology, University of Wisconsin. TIC: 237704.

Marshall, B.D. and Futa, K. 2001. "Strontium Isotope Evolution of Pore Water and Calcite in the Topopah Spring Tuff, Yucca Mountain, Nevada." *"Back to the Future—Managing the Back End of the Nuclear Fuel Cycle to Create a More Secure Energy Future," Proceedings of the 9th International High-Level Radioactive Waste Management Conference (IHLRWM), Las Vegas, Nevada, April 29–May 3, 2001.* La Grange Park, Illinois: American Nuclear Society. TIC: 247873.

Marshall, B.D.; Neymark, L.A.; Paces, J.B.; Peterman, Z.E.; and Whelan, J.F. 2000. "Seepage Flux Conceptualized from Secondary Calcite in Lithophysal Cavities in the Topopah Spring Tuff, Yucca Mountain, Nevada." *SME Annual Meeting, February 28–March 1, 2000, Salt Lake City, Utah.* Preprint 00-12. Littleton, Colorado: Society for Mining, Metallurgy, and Exploration. TIC: 248608.

Marshall, B.D. and Whelan, J.F. 2000. "Isotope Geochemistry of Calcite Coatings and the Thermal History of the Unsaturated Zone at Yucca Mountain, Nevada." *Abstracts with Programs—Geological Society of America, 32,* (7), A-259. Boulder, Colorado: Geological Society of America. TIC: 249113.

Marshall, B.D. and Whelan, J.F. (in press). "Simulating the Thermal History of the Unsaturated Zone at Yucca Mountain, Nevada." *Abstracts with Programs–Geological Society of America.* Boulder, Colorado: Geological Society of America.

Paces, J.B., Marshall, B.D., Whelan, J.F., Neymark, L.A., and Peterman, Z.E. 1998. *Summary of Subsurface Secondary Mineralization and Predictions of the Distribution and Isotopic Nature of Mineralization Along the East-West Cross-Drift Alignment, Yucca Mountain, Nevada.* Milestone SPC237M4. United States Geological Survey.

Paces, J.B., Neymark, L.A., Marshall, B.D., Whelan, J.F., and Peterman, Z.E. 2001. *Ages and Origins of Calcite and Opal in the Exploratory Studies Facility Tunnel, Yucca Mountain, Nevada.* Water-Resources Investigations Report 01-4049. Denver, Colorado: U.S. Geological Survey.

Pan, L. and Bodvarsson, G.S. 2001. *Modeling Transport in Fractured Porous Media with the Random-Walk Particle Method: The Transient Activity Range and the Particle-Transfer Probability.* LBNL-84042. Berkeley, California: Lawrence Berkeley National Laboratory. URN-0950

Philip, J.R.; Knight, J.H.; and Waechter, R.T. 1989. "Unsaturated Seepage and Subterranean Holes: Conspectus, and Exclusion Problem for Circular Cylindrical Cavities." *Water Resources Researc*h, *25,* (1), 16-28. Washington, D.C.: American Geophysical Union. TIC: 239117.

Pruess, K. and Narasimhan, T.N. 1985. "A Practical Method for Modeling Fluid and Heat Flow in Fractured Porous Media." *Society of Petroleum Engineers Journal, 25*, (1), 14-26. Dallas, Texas: Society of Petroleum Engineers. TIC: 221917.

Sonnenthal, E.L. and Bodvarsson, G.S. 1999. "Constraints on the Hydrology of the Unsaturated Zone at Yucca Mountain, NV from Three-Dimensional Models of Chloride and Strontium Geochemistry." *Journal of Contaminant Hydrology, 38,* (1-3), 107-156. New York, New York: Elsevier. TIC: 244160.

Triay, I.R.; Furlano, A.C.; Weaver, S.C.; Chipera, S.J.; and Bish, D.L. 1996. *Comparison of Neptunium Sorption Results Using Batch and Column Techniques.* LA-12958-MS. Los Alamos, New Mexico: Los Alamos National Laboratory. ACC: MOL.19980924.0049.

Whelan, J.F.; Roedder, E.; and Paces, J.B. 2001. "Evidence for an Unsaturated-Zone Origin of Secondary Minerals in Yucca Mountain, Nevada." *"Back to the Future—Managing the Back End of the Nuclear Fuel Cycle to Create a More Secure Energy Future," Proceedings of the 9th International High-Level Radioactive Waste Management Conference (IHLRWM), Las Vegas, Nevada, April 29-May 3, 2001.* La Grange Park, Illinois: American Nuclear Society. TIC: 247873.

Wilson, M.L. and Ho, C.K. 2001. "Abstraction of Seepage into Drifts." *"Back to the Future—Managing the Back End of the Nuclear Fuel Cycle to Create a More Secure Energy Future," Proceedings of the 9th International High-Level Radioactive Waste Management Conference (IHLRWM), Las Vegas, Nevada, April 29-May 3, 2001.* La Grange Park, Illinois: American Nuclear Society. TIC: 247873.

Wilson, S.F. and Cline, J.S. 2001. "Paragenesis, Temperature, and Timing of Secondary Minerals at Yucca Mountain." *"Back to the Future—Managing the Back End of the Nuclear Fuel Cycle to Create a More Secure Energy Future," Proceedings of the 9th International High-Level Radioactive Waste Management Conference (IHLRWM), Las Vegas, Nevada, April 29-May 3, 2001.* La Grange Park, Illinois: American Nuclear Society. TIC: 247873.

INTENTIONALLY LEFT BLANK